# Global Energy Efficiency in Secure MISO SWIPT Systems with Non-Linear Power-Splitting EH Model

Yang Lu, Ke Xiong, *Member, IEEE*, Pingyi Fan, *Senior Member, IEEE*, Zhiguo Ding, *Senior Member, IEEE*, Zhangdui Zhong, *Senior Member, IEEE*, Khaled Ben Letaief, *Fellow, IEEE*

***Abstract*—This paper considers a MISO simultaneous wireless information and power transfer (SWIPT) system where one transmitter serves multiple authorized receivers in presence of several potential eavesdroppers (idle receivers). To guarantee secure transmission, artificial noise (AN) is embedded into the transmit signals. The non-linear energy harvesting (EH) model is adopted and a novel power-splitting (PS) EH receiver architecture is proposed. The stochastic uncertainty channel model (SUM) is considered for the idle receivers due to outdated channel feedback. A global energy efficiency (GEE) maximization problem is formulated by jointly optimizing the transmit beamforming vectors and the AN covariance matrix at the transmitter and the PS ratios at idle receivers, under the minimal rate requirement and the secure transmission constraints of authorized receivers, the EH requirement constraints of idle receivers and the total available power constraint at the transmitter. To solve the non-convex optimization problem, an efficient solving approach is presented. Firstly, the PS ratios are optimized by using bisection method and successive convex approximation (SCA). Then, an iterative solution framework based on Dinkelbach's algorithm is presented to jointly optimize the transmit beamforming vectors and the AN covariance matrix, where a SCA-based algorithm is designed to solve its non-convex subproblem. It is theoretically proved that by involving the AN, the system GEE can be improved. Numerous results show that the system GEE first increases and then keeps unchanged with the increment of the total available power, and it first keeps unchanged and then decreases with the increment of the minimal rate requirement. It is also observed that compared with traditional EH receiver architecture and linear EH model, the proposed PS EH receiver architecture is able to achieve higher system GEE and avoid false output power at idle receivers.**

***Index Terms*—Energy efficiency, SWIPT, MISO, fractional programming, successive convex approximation, non-linear EH model, PS EH receiver architecture.**

Y. Lu and K. Xiong are with the School of Computer and Information Technology and also with the Beijing Key Lab of Traffic Data Analysis and Mining, Beijing Jiaotong University, Beijing, P. R. China, e-mail: kxiong@bjtu.edu.cn.

P. Y. Fan is with the National Laboratory for Information Science and Technology and also with Department of Electronic Engineering, Tsinghua University, Beijing, P. R. China.

Z. G. Ding is with School of Computing and Communications, Lancaster University, Lancaster, U.K. (e-mail: z.ding@lancaster.ac.uk).

Z. D. Zhong is with the State Key Laboratory of Rail Traffic Control and Safety and also with the Beijing Engineering Research Center of High-speed Railway Broadband Mobile Communications, Beijing Jiaotong University, Beijing, P. R. China.

K. B. Letaief is with the School of Engineering, Hong Kong University of Science and Technology (HKUST), Clear Water Bay, Hong Kong (e-mail: eekhaled@ece.ust.hk).

## I. Introduction

Recently, simultaneous wireless information and power transfer (SWIPT) has been regarded as one of the most promising technologies [1]–[4] since it utilizes radio frequency (RF) signals to realized dual functions, i.e., information decoding (ID) and energy harvesting (EH). For a SWIPT receiver, its electricity power could be charged by converting the received RF signals into required direct current (DC) power through EH circuits [5] and consequently, its operation time is prolonged. So, SWIPT offers great convenience to mobile users in 5G low-power energy-constrained networks such as wireless sensor networks (WSNs) and internet of things (IoTs). Therefore, lots of works focused on SWIPT-enabled WSN and IoT systems. For example, SWIPT was employed in multi-hop relaying networks in [6], [7] for WSNs and also was applied to charge wireless medical sensors in [8], [9] for IoTs.

To further improve the transmission efficiency, multi-antenna technology was integrated in SWIPT systems, since it is able to provide different services to different kinds of users over the same frequency band in one-time transmission. Since more and more privacy information is required to be delivered in some multi-antenna SWIPT systems [10], e.g., customized WSNs and IoTs, secure transmission becomes very essential. However, when security is taken into account, the system design becomes much more challengeable. The reason is that, in secure SWIPT networks, the received power at EH receivers need to be increased high enough to satisfy EH receivers' EH requirements, but in this case, the received signal-to-interference-noise ratio (SINR) at EH receivers is also enhanced, consequently, boosting the risk that the information for ID receivers intercepted by EH receivers. In order to reduce the risk and guarantee information security for ID receivers, one of the most efficient methods is to embed artificial noise (AN) into the transmit signals to cripple the information interception of the potential eavesdroppers [11], where the transmit beamforming vectors and AN covariance matrix are jointly generated to make the received SINR at EH receivers lower than a pre-defined threshold such that information cannot be correctly decoded.

On the other hand, as the energy consumption by information communications technology (ICT) industry increasing rapidly, green communications have become a basic requirement in future 5G communications [12]–[15]. To achieve green communications, developing energy efficient system designs

is of high significance, where power minimization [11] design aims at consuming as less energy as possible to stratify users' quality of service (QoS) requirements and energy efficiency (EE) maximization [16], [17] design intends to transmit as more bits as possible with per unit of energy consumption.

So far, multiple antennas, secure SWIPT and energy efficient system design have been widely studied in the literature (see e.g., [18]–[32]). Nevertheless, *only a few works have investigated them in a single communication system*. For example, the sum rate and the secrecy rate were respectively maximized for multi-user SWIPT systems in [18], [19] and in [20], [21], under available power and security constraints. However, their goals were to improve the system spectral efficiency (SE) rather than EE. As the energy consumption has become one of the most important issues in energy-constrained networks, more and more recent works began to study the energy efficient SWIPT system design, where works investigated the power minimization problem. For example, in [22] and [23], the total transmit power was minimized for cognitive radio and MIMO SWIPT networks, respectively, in order to save system energy with satisfying the receivers' QoS requirements. While other works investigated the EE maximization problem. For example, in [24]–[26], EE was maximized for cloud-based SWIPT networks and clustered WSNs, respectively, where transmitters were all equipped with single antenna. In order to inherit the benefits of multiple antennas, multi-antenna SWIPT system designs were investigated in many recent works, see e.g., [27] and [28], where the system EE was respectively maximized for MISO heterogeneous cellular networks in [27] and for MIMO two-way relay networks in [28]. However, the secure transmission issue was not considered in their works. To avoid information leakage, in [29], secrecy EE was maximized in MIMO multi-eavesdropper SWIPT networks but only the single-ID scenario was discussed. Compared with the single-ID receiver system, multi-ID receiver system is more difficult to design due to the interference among multiple users. In [30], secrecy rate and secrecy EE were maximized for multi-user MISO SWIPT networks, where however, only traditional linear EH model was adopted. As for the EH model, via real data measurement, recent research, see e.g., [31]–[36] documented that the RF-DC conversion efficiency of diode-based EH circuits is non-linear, and the analysis and transmit design with traditional linear EH model might result in inaccurate output and cause the system performance loss. Hence, more recent works designed the SWIPT system with the non-linear EH model proposed in [31], [32]. For example, in [31], outage probability for relay-aided SWIPT systems with non-linear energy harvester was analyzed, and in [32], max-sum resource allocation was present for downlink wireless powered networks under non-linear EH model.

In this paper, we investigate the EE for the AN-aided multi-user MISO SWIPT network with the non-linear EH model, where one transmitter serves multiple authorized receivers in presence of several potential eavesdroppers, i.e., idle receivers. The goal is to explore the system global EE (GEE) performance behavior. The contributions of this paper are summarized as follows.

- A novel PS EH receiver architecture is proposed which splits received RF signals into several streams and each stream is input into one EH circuit. The proposed architecture is motivated by the non-linear feature of diode-based EH circuits. That is, due to the reverse breakdown voltage of the diode included in EH circuits, the output DC power of one EH circuit cannot surpass its maximum limitation [33]–[36] (i.e., saturation status). When the EH circuit works in the saturation region, its RF-DC conversion efficiency decreases with the increment of the input RF power. With the proposed architecture, the power of each stream is made smaller than the total one, so by properly designing PS ratios associated with the streams, each EH circuit can be avoid working in the saturation region. Therefore, the RF-DC conversion efficiency of the EH circuit is improved, so is the system GEE. Note that although PS architecture was proposed in [1] and employed in many existing works, see e.g., [22], [24], their goal was to realize the simultaneous wireless ID and EH, while the PS architecture presented in our work is to improve the RF-DC conversion efficiency of the non-linear EH receivers.
- A GEE maximization problem is formulated by jointly optimizing the transmit beamforming vectors and the AN covariance matrix at the transmitter and the PS ratios at idle receivers, under the minimal rate requirement and the secure transmission constraints of authorized receivers, the EH requirement constraints of idle receivers and the total available power constraint at the transmitter. The stochastic uncertainty channel model (SUM) for the idle receivers is considered due to outdated channel feedback. Note that although the EE maximization problem has been studied for downlink MISO networks in the literature [37]–[40], SWIPT and secure transmission were not involved in a single system, and only the ideal perfect channel state information (CSI) assumption was considered. To the best of the authors' knowledge, this is the first work on investigating GEE maximization design for AN-aided multi-user MISO SWIPT system with the non-linear EH model and the SUM.
- Since the formulated GEE maximization problem is non-convex and cannot be solved directly due to its fractional objective function and probability constraints, in light of the intractability of the problem, an efficient solving approach is presented. Firstly, the PS ratios are optimized by using bisection method [19] and successive convex approximation (SCA) [41] to calculate the minimal required input RF power of each idle receiver. Then, an iterative solution framework based on Dinkelbach's algorithm [42]–[45] is presented to jointly optimize the transmit beamforming vectors and the AN covariance matrix, where a SCA-based algorithm is designed to solve its non-convex subproblem. Moreover, it is theoretically proved that by involving the AN, the system GEE can be improved.
- For comparison, the sum-rate maximization design and the power minimization design are also presented. Numerical results demonstrate that the proposed GEE maximization design is superior to the sum-rate maximization

design and the power minimization design in terms of GEE. In particular, the GEE of the sum-rate maximization design first increases and then decreases with the increment of the total available power while the GEE of the proposed GEE maximization design does not decrease. It is observed that, for relatively small available power, the GEE maximization design and the sum-rate maximization design achieve very similar system GEE. Moreover, the GEE of the power minimization design first increases and then decreases with the increment of the minimal rate requirement while the GEE of the proposed GEE maximization design first keeps unchanged and then decreased. For relatively high rate requirement, the GEE maximization design and the power minimization design achieve the similar system GEE. It is also observed that compared with traditional EH receiver architecture and linear EH model, the proposed PS EH receiver architecture is able to achieve higher system GEE and avoid false output power at idle receivers.

The remainder of the paper is organized as follows. Section II describes the system model, proposes the PS EH receiver architecture, and formulates an problem for the system. Section III presents a solving approach for the problem to explore the maximal GEE. The effect of AN is discussed in Section IV. Numerical results are provided in Section V and Section VI concludes this paper.

*Notations*: Boldface lowercase and uppercase letters denote vectors and matrices, respectively. The set of n-by-m real matrixes, complex matrixes and complex Hermitian matrixes are denoted by $\mathbb{R}^{n\times m}$, $\mathbb{C}^{n\times m}$ and $\mathbb{H}^{n\times m}$, respectively. For a complex number $a$, $|a|$ denotes the modulus. For a vector $\mathbf{a}$, $\|\mathbf{a}\|_2$ denotes the Euclidean norm. The conjugate transpose, rank, trace and determinant of the matrix $\mathbf{A}$ are denoted as $\mathbf{A}^H$, $\mathrm{Rank}\,(\mathbf{A})$, $\mathrm{Tr}\,(\mathbf{A})$ and $\det(\mathbf{A})$, respectively. $\mathbf{A}\succeq 0$ means $\mathbf{A}$ is a positive semidefinite (PSD) matrix. For a matrix $\mathbf{A}$, $s^-(\mathbf{A}) = \max\{\lambda_{\max}(-\mathbf{A}), 0\}$ and $s^+(\mathbf{A}) = \max\{\lambda_{\max}(\mathbf{A}), 0\}$. The symbol $\mathbf{I}$ denotes the identity matrix and $\mathbf{0}$ denotes a zero vector or matrix, The symbol $\mathbb{E}\{.\}$ represents the statistical expectation of the argument.

## II. System Model and Problem Formulation

### A. Network Model

Consider a downlink SWIPT network as shown in Figure 1, where a $N_{\mathrm{T}}$-antenna transmitter serves multiple energy-constrained legitimate receivers. The legitimate receivers are the users who are allowed to access the system frequency band. Considering that for some specific applications, not all legitimate receivers are authorized to decode the information associated with the applications, the legitimate receivers are classified into two types, i.e., the authorized receivers and the idle receivers. The authorized receiver is the paying user who is allowed to decode the information while the idle receiver is the non-paying user who is not allowed to decode the information. Nevertheless, the idle user is allowed to harvest energy from its collected signals. As a matter of fact, a legitimate receiver can be an authorized receiver for current transmission associated with an application but may become an idle receiver for the next transmission associated with the other applications. SWIPT technology is employed, so in each transmission, the transmitter delivers data to serve the authorized receivers while charging the idle receivers via the same transmit signals.

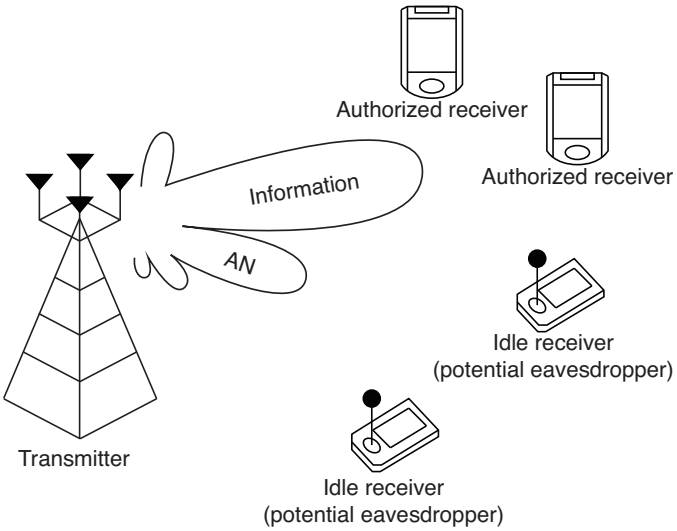


Fig. 1. Network model

It is assumed that there are $N$ authorized receivers and $K$ idle receivers in the system. For clarity, we use $n$ and $k$ to denote the $n$-th authorized receiver and the $k$-th idle receiver, respectively, where $n \in \mathcal{N} \triangleq \{1, 2, ..., N\}$ and $k \in \mathcal{K} \triangleq \{1, 2, ..., K\}$. All receivers are with single antenna, as in WSN and IoT scenarios, the receiver is often with very limited size to equip with multiple antennas. Note that the idle receivers may also have information decoding (ID) capability so they are able to eavesdrop the authorized receivers since all legitimate receivers are within the coverage of the transmitter. To prevent information leakage, the energy-bearing AN is embedded into the transmit signal.

### B. Channel Model and Information Transmission

Block flat fading channel is assumed, which means that the channel vectors remain constant within a block. Denote $\mathbf{h}_n \in \mathbb{C}^{N_{\mathrm{T}}\times 1}$ and $\mathbf{g}_k \in \mathbb{C}^{N_{\mathrm{T}}\times 1}$ to be the channel vectors from the transmitter to the $n$-th authorized receiver and the $k$-th idle receiver, respectively. As the authorized receivers report their CSI to the transmitter frequently during the transmission, perfect CSI is assumed for the authorized receivers. However, the CSI of the idle receivers may be outdated during the transmission since there is no interaction between the transmitter and the idle receivers. Therefore, imperfect CSI, i.e., SUM, is assumed for idle receivers, which is given by

$$\mathbf{g}_k = \hat{\mathbf{g}}_k + \mathbf{e}_k,$$

where $\hat{\mathbf{g}}_k \in \mathbb{C}^{N_{\mathrm{T}}\times 1}$ is the channel estimate of the $k$-th idle receiver and $\mathbf{e}_k \in \mathbb{C}^{N_{\mathrm{T}}\times 1}$ represents the channel error which is assumed to obey Gaussian distribution [46], i.e, $\mathbf{e}_k \sim \mathcal{CN}(\mathbf{0}, \mathbf{C}_k)$ with $\mathbf{C}_k \succeq \mathbf{0}$ denoting the covariance matrix.

In each time slot, the transmit signal at the transmitter consists the information signals for authorized receivers and the AN, which is given by

$$\mathbf{x} = \sum\nolimits_{n=1}^{N} \mathbf{w}_n \vartheta_n + \mathbf{z},$$

where $\vartheta_n \in \mathbb{C}$ denotes the symbol for the $n$-th authorized receiver, and without loss of generality, it is assumed that $\mathbb{E}\left\{|\vartheta_n|^2\right\} = 1$. $\mathbf{w}_n \in \mathbb{C}^{N_{\mathrm{T}} \times 1}$ is the beamforming vector associated with the $n$-th authorized receiver. $\mathbf{z} \in \mathbb{C}^{N_{\mathrm{T}} \times 1}$ indicates the energy-bearing AN with Gaussian distribution, i.e., $\mathbf{z} \sim \mathcal{CN}(\mathbf{0}, \mathbf{\Sigma})$ with $\mathbf{\Sigma} \succeq \mathbf{0}$. Then, the total required power of the transmitter is

$$P_{\mathrm{Total}}(\mathbf{w}_n, \mathbf{\Sigma}) = \mu \left( \sum\nolimits_{n=1}^{N} \|\mathbf{w}_n\|_2^2 + \mathrm{Tr}(\mathbf{\Sigma}) \right) + P_{\mathrm{c}},$$

where $\mu \in [1, \infty)$ is the power amplifier efficiency factor which is dependent of the information transmitting, and $P_{\mathrm{c}}$ is the circuit power consumed by the modules such as mixers, filters and digital-to-analog converters.

For the $n$-th authorized receiver, the received signal is given by

$$y_n = \mathbf{h}_n^H \mathbf{x} = \underbrace{\mathbf{h}_n^H \mathbf{w}_n \vartheta_n}_{\text{Desired signal}} + \underbrace{\sum\nolimits_{m \neq n}^{N} \mathbf{h}_n^H \mathbf{w}_m \vartheta_m}_{\text{Inter-receiver interference}} + \underbrace{\mathbf{h}_n^H \mathbf{z}}_{\text{AN}} + \underbrace{n_n}_{\text{AWGN}}, \quad (1)$$

where $n_n \sim \mathcal{CN}(0, \sigma^2)$ is the additive white Gaussian noises (AWGN) at the $n$-th authorized receiver with $\sigma^2$ denoting the noise power. Following (1), the achievable information rate at the $n$-th authorized receiver is given by

$$R_n(\mathbf{w}_n, \mathbf{\Sigma}) = \log\left(1 + \frac{\left|\mathbf{h}_n^H \mathbf{w}_n\right|^2}{\sum_{m \neq n}^{N} \left|\mathbf{h}_n^H \mathbf{w}_m\right|^2 + \mathbf{h}_n^H \mathbf{\Sigma} \mathbf{h}_n + \sigma^2}\right).$$

For the $k$-th idle receiver, the received signal is

$$y_k^{(\mathrm{Idle})} = \mathbf{g}_k^H \mathbf{x} = \sum\nolimits_{n=1}^{N} \mathbf{g}_k^H \mathbf{w}_n \vartheta_n + \mathbf{g}_k^H \mathbf{z} + n_k^{(\mathrm{Idle})} \quad (2)$$

where $n_k^{(\mathrm{Idle})} \sim \mathcal{CN}(0, \sigma^2)$ is the AWGN. If the $k$-th idle receiver intends to intercept the information for the $n$-th authorized receiver, following (2), its received signal-interference-to-noise-ratio (SINR) is given by

$$\Gamma_{k,n}^{(\mathrm{Idle})}(\mathbf{w}_n, \mathbf{\Sigma}) = 1 + \frac{\left|\mathbf{g}_k^H \mathbf{w}_n\right|^2}{\sum_{m \neq n}^{N} \left|\mathbf{g}_k^H \mathbf{w}_m\right|^2 + \mathbf{g}_k^H \mathbf{\Sigma} \mathbf{g}_k + \sigma^2}.$$

### *C. Non-linear EH Model and Our Proposed PS EH Receiver Architecture*

Although the idle receivers are not allowed to decode information, they are legitimate receivers for EH. The received power carried in the received RF signals at the $k$-th idle receiver is

$$P_k(\mathbf{w}_n, \mathbf{\Sigma}) = \mathbf{g}_k^H \left( \sum\nolimits_{n=1}^{N} \mathbf{w}_n \mathbf{w}_n^H + \mathbf{\Sigma} \right) \mathbf{g}_k.$$

As the practical EH circuit includes various non-linearities, such as the diode, its RF-DC conversion efficiency depends on the input RF power level. That is, it is with non-linear features. As illustrated in Figure 2(a), different from traditional linear EH model, the output DC power of the non-linear EH model cannot surpass the limitation on the maximum output DC power due to the reverse breakdown voltage of the diode [33]–[36]. That is, when the output DC power reaches the saturation region, the RF-DC conversion efficiency of the non-linear EH model decreases with the increment of the input RF power in Figure 2(b). It is seen that the linear EH model is much different from the practical non-linear EH model, so if the linear EH model is adopted for system design, the caused mismatch cannot be neglected. Therefore, in this paper, we consider the non-linear EH model.

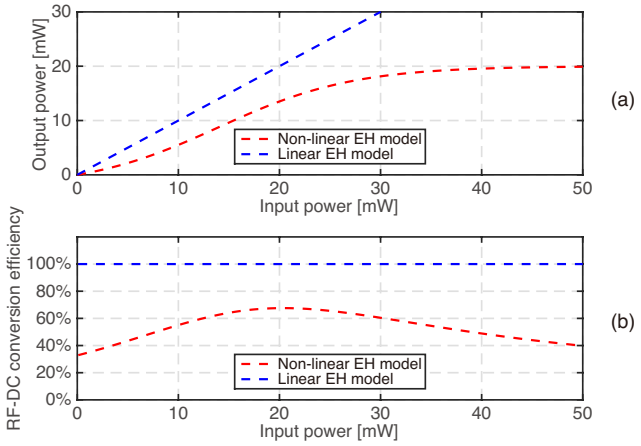


Fig. 2. (a) The output DC power versus the input RF power of the non-linear EH model. (b) The RF-DC conversion efficiency versus the input RF power of the non-linear EH model.

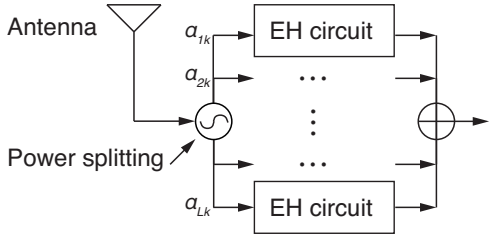


Fig. 3. The proposed PS EH receiver architecture at the $k$-th idle receiver.

From the non-linear EH model, it also can be observed that when the circuit works in the saturation region, the input RF power is wasted, which is converted with low efficiency. To avoid an EH circuit entering into the saturation region, we propose a PS EH receiver architecture, as shown in Figure 3, by employing $L$ EH circuits, with which the received RF signals are split into $L$ streams and each stream is input into one EH circuit. As the power of each stream is smaller than the total one, by properly splitting the streams, each EH circuit can be avoid working in the saturation region[1]. Let $\alpha_{kl}$ denote the PS ratio for the $l$-th EH circuit at the $k$-th idle receiver. It

[1]The proposed PS EH receiver architecture is similar to the one presented in [1]. The difference is that the PS receiver in [1] was used for simultaneous ID and EH in SWIPT, but ours is designed for EH.

satisfies that

$$\sum\nolimits_{l=1}^{L} \alpha_{kl} = 1,\ \forall k \in \mathcal{K}.$$

Thus, the total harvested power (i.e., output DC power) at the $k$-th idle receiver with our proposed PS EH receiver architecture under the non-linear EH model can be given by

$$\Phi_k\left(P_k\left(\mathbf{w}_n, \mathbf{\Sigma}\right), \{\alpha_{kl}\}\right) = \sum_{l=1}^{L}\left(\frac{M_{kl}}{X_{kl}\left(1+\exp\left(-\upsilon_{kl}\left(\alpha_{kl}P_k\left(\mathbf{w}_n, \mathbf{\Sigma}\right)-\varphi_{kl}\right)\right)\right)} - Y_{kl}\right)$$

where $X_{kl} = \frac{\exp(\upsilon_{kl}\varphi_{kl})}{1+\exp(\upsilon_{kl}\varphi_{kl})}$ and $Y_{kl} = \frac{M_{kl}}{\exp(\upsilon_{kl}\varphi_{kl})}$. $M_{kl}$, $\upsilon_{kl}$ and $\varphi_{kl}$ are constants. $M_{kl}$ denotes the maximum limitation on output DC power while $\upsilon_{kl}$ and $\varphi_{kl}$ represent the resistance, the capacitance and the circuit sensitivity. *Note that the traditional EH receiver architecture can be regards a special case of our proposed PS EH receiver architecture by inputing all received RF signals into one EH circuit.*

### D. Problem Formulation

For the considered system, the GEE (measured in bits/Hz/J) is defined as the ratio of sum rate of the authorized receivers and the total required power,

$$\mathrm{GEE}\left(\mathbf{w}_n, \mathbf{\Sigma}\right) = \frac{\sum_{n=1}^{N} R_n\left(\mathbf{w}_n, \mathbf{\Sigma}\right)}{P_{\mathrm{Total}}\left(\mathbf{w}_n, \mathbf{\Sigma}\right)}.$$

The proposed system design aims at maximizing the system GEE while satisfying the minimal rate requirement and the secure transmission constraints of authorized receivers, the EH requirement constraints of idle receivers and the total available power constraint at the transmitter. Denoting $\mathbf{\Lambda} = [\alpha_{kl}]_{k,l} \in \mathbb{R}^{K\times L}$, the considered problem is mathematically expressed as the following Problem $\mathrm{P}_0$.

$$\begin{aligned}
\mathbf{P_0}: \max_{\{\mathbf{w}_n, \mathbf{\Sigma}, \mathbf{\Lambda}\}} \ & \mathrm{GEE}\left(\mathbf{w}_n, \mathbf{\Sigma}\right) && \text{(3a)}\\
\text{s.t. } & R_n\left(\mathbf{w}_n, \mathbf{\Sigma}\right) \geq R_n^{(\mathrm{D})}, && \text{(3b)}\\
& P_{\mathrm{Total}}\left(\mathbf{w}_n, \mathbf{\Sigma}\right) \leq P_{\mathrm{Max}} && \text{(3c)}\\
& \Pr\left\{\Phi_k\left(P_k\left(\mathbf{w}_n, \mathbf{\Sigma}\right), \{\alpha_{kl}\}\right) \geq \theta_k\right\} \geq 1 - p_k^{(\mathrm{EH})}, && \text{(3d)}\\
& \Pr\left\{\Gamma_{k,n}^{(\mathrm{Idle})}\left(\mathbf{w}_n, \mathbf{\Sigma}\right) \leq \Gamma_{\mathrm{E}}\right\} \geq 1 - p_{k,n}^{(\mathrm{ID})}, && \text{(3e)}\\
& \sum\nolimits_{l=1}^{L} \alpha_{kl} = 1, && \text{(3f)}\\
& \mathbf{\Sigma} \succeq \mathbf{0},\ \forall n \in \mathcal{N},\ \forall k \in \mathcal{K}. && \text{(3g)}
\end{aligned}$$

In (3b), $R_n^{(\mathrm{D})}$ is the minimum required rate of the $n$-th authorized receiver. In (3c), $P_{\mathrm{Max}}$ is the total available power. In (3d), $\theta_k$ is the EH requirement at the $k$-th idle receiver. Since only outdated CSI of the idle receiver is available at the transmitter as mentioned previously, the EH requirement can only be guaranteed in portability. Therefore, $p_k^{(\mathrm{EH})} \in (0, 1]$ denotes the tolerable outage probability threshold for the $k$-th idle receiver, which implies that the EH requirement satisfaction probability should be kept no less than $1 - p_k^{(\mathrm{EH})}$. In (3e), $\Gamma_k^{(\mathrm{E})}$ is the SINR threshold for successfully decoding information, which means that when the received SINR at $k$-th idle receiver associated with the $n$-th authorized receiver ($\forall n \in \mathcal{N}$) is lower than $\Gamma_k^{(\mathrm{E})}$, the $k$-th idle receiver cannot decode and eavesdrop the information. With such a constraint, the information interception can be prevented [11]. $p_{k,n}^{(\mathrm{ID})} \in (0, 1]$ denotes the tolerable security probability threshold, which implies that the information security is guaranteed with a probability no less than $1 - p_{k,n}^{(\mathrm{ID})}$.

It is seen that Problem $\mathrm{P}_0$ is not convex and cannot be solved with traditional methods, due to the fractional objective function and the outage constraints. Hence, we design an efficient solving approach for it in Section III.

## III. Solving Approach

Problem $\mathrm{P}_0$ is solved with the following idea. First, we optimize $\mathbf{\Lambda}$ for the proposed PS EH receiver architecture as the optimization of $\mathbf{\Lambda}$ is dependent of the optimization of $\{\mathbf{w}_n, \mathbf{\Sigma}\}$. This is because with a given EH receiver architecture and a EH requirement $\theta_k$, the minimal required input RF power of the $k$-th idle receiver to satisfy (3d) is determined. Thus, we just need to optimize $\{\mathbf{w}_n, \mathbf{\Sigma}\}$ to satisfy the minimal required input RF power of the $k$-th idle receiver ($\forall k \in \mathcal{K}$). Then, with the optimal $\mathbf{\Lambda}^\star$, we recast the fractional objective function of considered problem as the difference of its numerator and denominator according to fractional programming. An iterative algorithm is designed based on a generalized Dinkelbach's algorithm to optimize $\{\mathbf{w}_n, \mathbf{\Sigma}\}$. However, as the Dinkelbach's algorithm still cannot be applied directly due to our considered problem in each iteration including a non-convex subproblem. A convex approximation formulation is presented to deal with the non-convex subproblem by using semi-definition relaxation (SDR), Bernstein-type inequality and first-order approximation techniques, and a SCA-based algorithm is designed to improve the approximating precision. The detail process of our proposed solution method are described as follows.

### A. Optimization of $\mathbf{\Lambda}$

With a given EH requirement $\theta_k$, the optimization of $\{\alpha_{kl}^\star\}_l$ is independent of the optimization $\{\mathbf{w}_n, \mathbf{\Sigma}\}$, so it is optimized at first. For the $k$-th idle receiver, we define $\mathcal{E}_k$ to denote its required input RF power. The optimal PS ratios $\{\alpha_{kl}^\star\}_l$ must yield the minimal $\mathcal{E}_k$. Therefore, we formulate Problem $\mathrm{P}_\Lambda$ to find the optimal $\{\alpha_{kl}^\star\}_l$ by minimizing $\mathcal{E}_k$.

$$\begin{aligned}
\mathbf{P_\Lambda}: \min_{\{\alpha_{kl}, \mathcal{E}_k\}} \ & \mathcal{E}_k && \text{(4a)}\\
\text{s.t. } & \Phi_k\left(\mathcal{E}_k, \{\alpha_{kl}\}\right) \geq \theta_k,\ \text{(3f)}, && \text{(4b)}
\end{aligned}$$

By introducing slack variables $\{\kappa_{kl}\}_l$ ($l \in [1, ..., L]$), solving Problem $\mathrm{P}_\Lambda$ is equivalent to solving the following Problem $\mathrm{P}_{\Lambda-1}$.

$$\begin{aligned}
\mathbf{P_{\Lambda-1}}: \min_{\{\alpha_{kl}, \mathcal{E}_k, \kappa_{kl}\}} \ & \mathcal{E}_k && \text{(5a)}\\
\text{s.t. } & \text{(3f)}, && \text{(5b)}\\
& \sum\nolimits_{l=1}^{L} \kappa_{kl} \geq \theta_k, && \text{(5c)}\\
& \frac{M_{kl}}{\kappa_{kl} + Y_{kl}} \geq X_{kl}\left(1+\exp\left(-\upsilon_{kl}\left(\alpha_{kl}\mathcal{E}_k - \varphi_{kl}\right)\right)\right). && \text{(5d)}
\end{aligned}$$

It can be observed that in Problem $\mathrm{P}_{\Lambda-1}$, constraint (5d) is non-convex which cannot be dealt with directly. For a fixed $\mathcal{E}_k$, a feasibility problem associated with Problem $\mathrm{P}_{\Lambda-1}$ is given by Problem $\mathrm{P}_{\Lambda-2}$ which aims to find a feasible $\{\alpha_{kl}, \kappa_{kl}\}$ such that constraints (3f), (5c) and (5d) are all satisfied. With the decrement of $\mathcal{E}_k$, one can keep solving Problem $\mathrm{P}_{\Lambda-2}$ until $\mathrm{P}_{\Lambda-2}$ is infeasible. The last $\mathcal{E}_k$ corresponding a feasible Problem $\mathrm{P}_{\Lambda-2}$ must be the minimal $\mathcal{E}_k^\star$. Although such a solving idea is intuitive, it is inefficient, because it may require exhaustive search.

$$\mathbf{P_{\Lambda-2}}: \text{find} \{\alpha_{kl}, \kappa_{kl}\} \quad \text{s.t. (3f), (5c), (5d).} \tag{6a}$$

Therefore, we solve Problem $\mathrm{P}_{\Lambda-2}$ by considering the following $\mathrm{P}_{\Lambda-3}$ instead. For a given $\mathcal{E}_k$, the maximum $\sum_{l=1}^{L} \kappa_{kl}$ can be obtained by solving $\mathrm{P}_{\Lambda-3}$. If the obtained maximum $\sum_{l=1}^{L} \kappa_{kl}$ is less than $\theta_k$, the corresponding optimal solution of Problem $\mathrm{P}_{\Lambda-3}$ is infeasible to Problem $\mathrm{P}_{\Lambda-2}$. Otherwise, it is feasible to Problem $\mathrm{P}_{\Lambda-2}$. Therefore, we design a bisection-method based algorithm to find the minimal $\mathcal{E}_k^\star$ by solving Problem $\mathrm{P}_{\Lambda-3}$ as shown in Algorithm 1, where $\iota$ and $u$ is the lower bound and upper bound of received RF power, respectively, and $\varepsilon$ is a small positive number.

$$\mathbf{P_{\Lambda-3}}: \max_{\{\alpha_{kl}, \kappa_{kl}\}} \sum_{l=1}^{L} \kappa_{kl} \quad \text{s.t. (3f), (5d).} \tag{7a}$$

Note that since Problem $\mathrm{P}_{\Lambda-3}$ still cannot be solved directly due to non-convexity of (5d), we transform Problem $\mathrm{P}_{\Lambda-3}$ to Problem $\mathrm{P}_{\Lambda-4}$ by approximating (5d) with its lower bound as follows.

It is observed that the left-hand side of (5d) is a convex function. By first-order approximation, the lower bound of $\frac{M_{kl}}{\kappa_{kl}+Y_{kl}}$ at a feasible $\bar{\kappa}_{kl}$ is given by

$$\frac{M_{kl}}{\bar{\kappa}_{kl}+Y_{kl}} - \frac{M_{kl}}{\left(\bar{\kappa}_{kl}+Y_{kl}\right)^2}\left(\kappa_{kl}-\bar{\kappa}_{kl}\right).$$

Then, (5d) is relaxed to be

$$\frac{M_{kl}}{\bar{\kappa}_{kl}+Y_{kl}} - \frac{M_{kl}}{\left(\bar{\kappa}_{kl}+Y_{kl}\right)^2}\left(\kappa_{kl}-\bar{\kappa}_{kl}\right) \geq X_{kl}\left(1+\exp\left(-\upsilon_{kl}\left(\alpha_{kl}\mathcal{E}_k-\varphi_{kl}\right)\right)\right). \tag{8}$$

By replacing (5d) with (8), Problem $\mathrm{P}_{\Lambda-3}$ is approximately formulated as the following Problem $\mathrm{P}_{\Lambda-4}$.

$$\mathbf{P_{\Lambda-4}}: \max_{\{\alpha_{kl}, \kappa_{kl}\}} \sum_{l=1}^{L} \kappa_{kl} \quad \text{s.t. (3f), (8).} \tag{9a}$$

Problem $\mathrm{P}_{\Lambda-4}$ is convex which can be solved by using standard convex optimization solvers, e.g., SeduMi or CVX [47]. But due to the relaxation from Problem $\mathrm{P}_{\Lambda-3}$ to Problem $\mathrm{P}_{\Lambda-4}$, the optimal solution to Problem $\mathrm{P}_{\Lambda-4}$ may not be precise to Problem $\mathrm{P}_{\Lambda-3}$. Therefore, we use SCA to improve the precision, which is described in detail by the inner iteration in Algorithm 1. With above process, the optimal $\mathbf{\Lambda}^\star$ is obtained, so is the optimal $\mathcal{E}_k^\star$.

**Algorithm 1** Optimization of $\mathbf{\Lambda}$

1: **Initialize** $\iota \leq \mathcal{E}_k^\star \leq u$;
2: **repeat**
3: Update $\ell$=$(\iota+u)/2$;
4: **repeat**
5: Initialize $\{\bar{\kappa}_{kl}(0)\}$ and set $t=1$;
6: Obtain $\{\kappa_{kl}^\star(t)\}$ by solving Problem $\mathrm{P}_{\Lambda-4}$;
7: Update $\{\bar{\kappa}_{kl}(t)\} = \{\kappa_{kl}^\star(t)\}$;
8: $t = t+1$;
9: **until** $\sum_{l=1}^{L}\kappa_{kl}^\star(t) - \sum_{l=1}^{L}\kappa_{kl}^\star(t-1) \leq \varepsilon$;
10: If $\sum_{l=1}^{L}\kappa_{kl}^\star(t) > \theta_k$, update $\iota = \ell$; otherwise update $u = \ell$;
11: **until** $u - \iota < \varepsilon$;
12: **return** $\{\alpha_{kl}^\star, \mathcal{E}_k^\star\}$.

### B. Optimization of $\{\mathbf{w}_n, \mathbf{\Sigma}\}$

*1) Iterative Solution Framework based on Dinkelbach's Algorithm :* With $\mathcal{E}_k^\star$, we can optimize $\{\mathbf{w}_n, \mathbf{\Sigma}\}$ by solving the following Problem $\mathrm{P}_1$ instead of Problem $\mathrm{P}_0$.

$$\mathbf{P_1}: \max_{\{\mathbf{w}_n, \mathbf{\Sigma}\}} \mathrm{GEE}(\mathbf{w}_n, \mathbf{\Sigma}) \tag{10a}$$

$$\text{s.t. } \Pr\left\{\mathbf{g}_k^H\left(\sum\nolimits_{n=1}^{N}\mathbf{w}_n^H + \mathbf{\Sigma}\right)\mathbf{g}_k + \sigma^2 \geq \mathcal{E}_k^\star\right\} \geq 1 - p_k^{(\mathrm{EH})}, \tag{10b}$$

$$\text{(3b), (3c), (3e), (3g).}$$

As the fractional function, i.e., $\mathrm{GEE}(\mathbf{w}_n, \mathbf{\Sigma})$, is neither convex nor concave, standard convex optimization algorithms cannot be applied. Nevertheless, according to the fractional programming [42]–[45], Dinkelbach's algorithm may be employed to globally maximize the fractional function with polynomial complexity.

**Lemma 1.** [42] *The optimal solution $\{\mathbf{w}_n^\star, \mathbf{\Sigma}^\star\}$ to Problem $P_1$ can be achieved if and only if $\lambda^\star$ being the unique zero of the auxiliary function $F(\lambda)$ where*

$$F(\lambda) \triangleq \sum\nolimits_{n=1}^{N} R_n(\mathbf{w}_n, \mathbf{\Sigma}) - \lambda P_{\mathrm{Total}}(\mathbf{w}_n, \mathbf{\Sigma}).$$

*Proof:* The proof of Lemma 1 can be found in [42], which is omitted here. ■

With Lemma 1, instead of solving Problem $\mathrm{P}_1$, we solve the following auxiliary Problem $\mathrm{P}_2$ to find the optimal $\{\mathbf{w}_n^\star, \mathbf{\Sigma}^\star\}$, as it has the same optimal solution with Problem $\mathrm{P}_1$.

$$\mathbf{P_2}: \max\nolimits_{\{\mathbf{w}_n, \mathbf{\Sigma}, \lambda\}} F(\lambda) \quad \text{s.t. (3b), (3c), (3e), (3g), (10b).}$$

Problem $\mathrm{P}_2$ can be solved by using a generalized Dinkelbach's algorithm which is described by Algorithm 2, where the key step is the step 4, i.e., how to solve the following Problem $\mathrm{P}_3$.

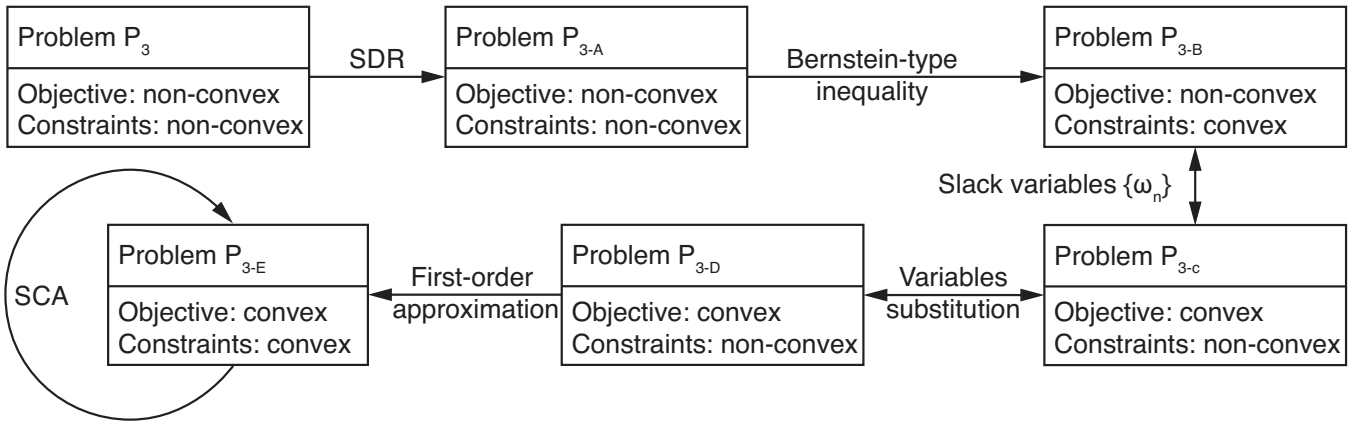


Fig. 4. Solving ideal for Problem $\mathrm{P}_3$.

**Algorithm 2** Iterative solution framework based on Dinkelbach's algorithm for solving Problem $\mathrm{P}_2$

1: Initialize $\lambda(0)$ with $F(\lambda(0)) \geq 0$;
2: Set $p = 0$;
3: **repeat**
4: Obtain $\{(\mathbf{w}_n^\star(q), \mathbf{\Sigma}^\star(q))\}$ by Solving Problem $\mathrm{P}_3$;
5: Update $F(\lambda(q)) = \sum_{n=1}^{N} R_n(\mathbf{w}_n^\star(q), \mathbf{\Sigma}^\star(q)) - \lambda(q) P_{\mathrm{Total}}(\mathbf{w}_n^\star(q), \mathbf{\Sigma}^\star(q))$;
6: Update

$$\lambda(q+1) = \frac{\sum_{n=1}^{N} R_n(\mathbf{w}_n^\star, \mathbf{\Sigma}^\star)}{P_{\mathrm{Total}}(\mathbf{w}_n^\star(q), \mathbf{\Sigma}^\star(q))};$$

7: $q = q + 1$;
8: **until** $F(\lambda(q)) < \varepsilon$.

$$\mathbf{P_3}: \max_{\{\mathbf{w}_n, \mathbf{\Sigma}\}} F(\lambda(q))$$
$$\text{s.t. (3b), (3c), (3e), (3g), (10b).}$$

Since Problem $\mathrm{P}_3$ is non-convex, which is difficult to deal with. Therefore, we design an algorithm for Problem $\mathrm{P}_3$ as follows.

*2) SCA-Based Algorithm for Problem $P_3$ :* Before giving the detailed algorithm of Problem $\mathrm{P}_3$, for the readers' convenience, we summarize the solving idea in Figure 4, where Problem $\mathrm{P}_3$ is approximated by Problem $\mathrm{P}_{3-\mathrm{E}}$ via several steps of transformation based on SDR, Bernstein-type inequality and first-order approximation techniques. Then, a SCA-based algorithm is presented to improve the approximation precision.

By defining $\mathbf{W}_n = \mathbf{w}_n \mathbf{w}_n^H$, the rate of the $n$-th authorized receiver, the received SINR at the $k$-th idle receiver on eavesdropping the $n$-th authorized receiver and the total required power can be respectively given by

$$R_n(\mathbf{W}_n, \mathbf{\Sigma}) = \log\left(1 + \frac{\mathbf{h}_n^H \mathbf{W}_n \mathbf{h}_n}{\sum_{m \neq n}^{N} \mathbf{h}_n^H \mathbf{W}_m \mathbf{h}_n + \mathbf{h}_n^H \mathbf{\Sigma} \mathbf{h}_n + \sigma^2}\right),$$

$$\Gamma_{k,n}^{(\mathrm{Idle})}(\mathbf{W}_n, \mathbf{\Sigma}) = \frac{\mathbf{g}_k^H \mathbf{W}_n \mathbf{g}_k}{\sum_{m \neq n}^{N} \mathbf{g}_k^H \mathbf{W}_m \mathbf{g}_k + \mathbf{g}_k^H \mathbf{\Sigma} \mathbf{g}_k + \sigma^2},$$

and

$$P_{\mathrm{Total}}(\mathbf{W}_n, \mathbf{\Sigma}) = \mu \mathrm{Tr}\left(\sum_{n=1}^{N} \mathbf{W}_n + \mathbf{\Sigma}\right) + P_{\mathrm{c}}.$$

Note that $\mathbf{W}_n = \mathbf{w}_n \mathbf{w}_n^H$ is a equivalent transformation if and only if $\mathrm{Rank}(\mathbf{W}_n) = 1$. However, $\mathrm{Rank}(\mathbf{W}_n) = 1$ is not a convex constraint. By dropping $\mathrm{Rank}(\mathbf{W}_n) = 1$, the SDR form of Problem $\mathrm{P}_3$ can be given by the following Problem $\mathrm{P}_{3-\mathrm{A}}$, where for notational simplicity, we omit the iteration index $q$.

$$\begin{aligned}
\mathbf{P_{3-A}}: & \max_{\{\mathbf{W}_n, \mathbf{\Sigma}\}} \sum_{n=1}^{N} R_n(\mathbf{W}_n, \mathbf{\Sigma}) - \lambda P_{\mathrm{Total}}(\mathbf{W}_n, \mathbf{\Sigma}) \\
& \text{s.t. } \mathbf{h}_n^H \mathbf{W}_n \mathbf{h}_n && \text{(11a)} \\
& \quad \geq \left(2^{R_n^{(\mathrm{D})}} - 1\right)\left(\sum_{m \neq n}^{N} \mathbf{h}_n^H \mathbf{W}_m \mathbf{h}_n + \mathbf{h}_n^H \mathbf{\Sigma} \mathbf{h}_n + \sigma^2\right), \\
& \quad \mu \mathrm{Tr}\left(\sum_{n=1}^{N} \mathbf{W}_n + \mathbf{\Sigma}\right) + P_{\mathrm{c}} \leq P_{\mathrm{Max}}, && \text{(11b)} \\
& \quad \Pr\left\{\mathbf{g}_k^H \left(\sum_{n=1}^{N} \mathbf{W}_n^H + \mathbf{\Sigma}\right) \mathbf{g}_k + \sigma^2 \geq \mathcal{E}_k^\star\right\} \geq 1 - p_k^{(\mathrm{EH})}, && \text{(11c)} \\
& \quad \Pr\left\{\Gamma_{k,n}^{(\mathrm{Idle})}(\mathbf{W}_n, \mathbf{\Sigma}) \leq \Gamma_{\mathrm{E}}\right\} \geq 1 - p_{k,n}^{(\mathrm{ID})}, && \text{(11d)} \\
& \quad \mathbf{W}_n \succeq \mathbf{0},\ \mathbf{\Sigma} \succeq \mathbf{0},\ \forall n \in \mathcal{N},\ \forall k \in \mathcal{K}. && \text{(11e)}
\end{aligned}$$

As the outage constraints (11c) and (11d) have no explicit expressions. To solve it, Bernstein-type inequality is employed based on the following Lemma 2.

**Lemma 2.** [48] *Given* $\mathbf{e} \sim \mathcal{CN}(\mathbf{0}, \mathbf{I}_n)$, $\mathbf{Q} \in \mathbb{C}^{n \times n}$ *and* $\mathbf{r} \in \mathbb{C}^{n \times 1}$, *for any* $\eta_1, \eta_2 > 0$, *it holds that*

$$\mathrm{Prob}\left\{\mathbf{e}^H \mathbf{Q} \mathbf{e} + 2\mathrm{Re}\left\{\mathbf{e}^H \mathbf{r}\right\} \geq \Upsilon_1(\eta_1)\right\} \geq 1 - e^{-\eta_1},$$

*and*

$$\mathrm{Prob}\left\{\mathbf{e}^H \mathbf{Q} \mathbf{e} + 2\mathrm{Re}\left\{\mathbf{e}^H \mathbf{r}\right\} \leq \Upsilon_2(\eta_2)\right\} \geq 1 - e^{-\eta_2}$$

*where*

$$\Upsilon_1(\eta_1) = \mathrm{Tr}(\mathbf{Q}) - \sqrt{2\eta}\sqrt{\|\mathbf{Q}\|_F^2 + 2\|\mathbf{r}\|^2} - \eta s^-(\mathbf{Q}),$$

*and*

$$\Upsilon_2(\eta_2) = \mathrm{Tr}(\mathbf{Q}) + \sqrt{2\eta}\sqrt{\|\mathbf{Q}\|_F^2 + 2\|\mathbf{r}\|^2} + \eta s^+(\mathbf{Q}).$$

*Proof:* The proof of Lemma 2 can be referred to [48], which is omitted here. ■

Before applying Lemma 2, we rewrite $\mathbf{e}_k$ as $\mathbf{e}_k = \mathbf{C}_k^{1/2}\mathbf{v}_k$, where $\mathbf{C}_k^{1/2} \succeq \mathbf{0}$ is the PSD square roots of $\mathbf{C}_k$ and $\mathbf{v}_k \sim \mathcal{CN}(\mathbf{0}, \mathbf{I}_{N_\mathrm{t}})$. By defining $\delta_k = -\ln\left(p_k^{(\mathrm{EH})}\right)$ and $\varsigma_{k,n} = -\ln\left(p_{k,n}^{(\mathrm{ID})}\right)$, (11c) and (11d) can be rewritten as

$$\Pr\left\{\mathbf{v}_n^H\boldsymbol{\Theta}_k\mathbf{v}_k + 2\mathrm{Re}\left\{\boldsymbol{\omega}_k^H\mathbf{v}_k\right\} + \sigma^2 \geq \mathcal{E}_k^\star - s_k\right\} \geq 1 - e^{-\delta_k} \tag{12}$$

and

$$\Pr\left\{\mathbf{v}_n^H\boldsymbol{\Theta}_{k,n}\mathbf{v}_k + 2\mathrm{Re}\left\{\boldsymbol{\omega}_{k,n}^H\mathbf{v}_k\right\} \leq \Gamma_\mathrm{E}\sigma^2 - s_{k,n}\right\} \geq 1 - e^{-\varsigma_k} \tag{13}$$

where

$$\begin{cases} \boldsymbol{\Theta}_k = \mathbf{C}_k^{1/2}\mathbf{M}\mathbf{C}_k^{1/2},\ \boldsymbol{\omega}_k = \mathbf{C}_k^{1/2}\mathbf{M}\hat{\mathbf{g}}_k,\ s_k = \hat{\mathbf{g}}_k^H\mathbf{M}\hat{\mathbf{g}}_k, \\ \boldsymbol{\Theta}_{k,n} = \mathbf{C}_k^{1/2}\mathbf{T}_n\mathbf{C}_k^{1/2},\ \boldsymbol{\omega}_{k,n} = \mathbf{C}_k^{1/2}\mathbf{T}_n\hat{\mathbf{g}}_k, \\ s_{k,n} = \hat{\mathbf{g}}_k^H\mathbf{T}_n\hat{\mathbf{g}}_k,\ \mathbf{M} = \left(\sum_{n=1}^N \mathbf{W}_n^H + \boldsymbol{\Sigma}\right), \\ \mathbf{T}_n = \left(\mathbf{W}_n - \Gamma_\mathrm{E}\left(\sum_{n\neq m}^N \mathbf{W}_n + \boldsymbol{\Sigma}\right)\right). \end{cases}$$

In terms of Lemma 2, the inequalities (12) and (13) hold true if the following inequalities, i.e.,

$$\begin{aligned} &\mathrm{Tr}\left(\boldsymbol{\Theta}_k\right) - \sqrt{2\delta_k}\sqrt{\left\|\boldsymbol{\Theta}_k\right\|_F^2 + 2\left\|\boldsymbol{\omega}_k\right\|^2} - \delta_k s^-\left(\boldsymbol{\Theta}_k\right) \\ &\geq \mathcal{E}_k^\star - s_k - \sigma^2 \end{aligned} \tag{14}$$

and

$$\begin{aligned} &\mathrm{Tr}\left(\boldsymbol{\Theta}_{k,n}\right) + \sqrt{2\varsigma_k}\sqrt{\left\|\boldsymbol{\Theta}_{k,n}\right\|_F^2 + 2\left\|\boldsymbol{\omega}_{k,n}\right\|^2} + \varsigma_k s^+\left(\boldsymbol{\Theta}_{k,n}\right) \\ &\leq \Gamma_\mathrm{E}\sigma^2 - s_{k,n} \end{aligned} \tag{15}$$

are satisfied at the same time.

By introducing two auxiliary variables $x_k$ and $y_k$, constraint (14) can be equivalently transformed into a group of inequalities in (16), i.e.,

$$\begin{cases} \mathrm{Tr}\left(\boldsymbol{\Theta}_k\right) - \sqrt{2\delta_k}x_k - \delta_k y_k \geq \mathcal{E}_k^\star - s_k - \sigma^2, \\ \left\|\left[\mathbf{vec}(\boldsymbol{\Theta}_k)^H\ \sqrt{2}\boldsymbol{\omega}_k^H\right]\right\|_2 \leq x_k, \\ y_k\mathbf{I} + \boldsymbol{\Theta}_k \succeq \mathbf{0}, \\ y_k \geq 0. \end{cases} \tag{16}$$

Similarly, with another two auxiliary variables $x_{k,n}$ and $y_{k,n}$, constraint (15) can be equivalently transformed to be

$$\begin{cases} \mathrm{Tr}\left(\boldsymbol{\Theta}_{k,n}\right) + \sqrt{2\varsigma_k}x_{k,n} + y_{k,n} \leq \Gamma_\mathrm{E}\sigma^2 - s_{k,n}, \\ \left\|\left[\mathbf{vec}(\boldsymbol{\Theta}_{k,n})^H\ \sqrt{2}\boldsymbol{\omega}_{k,n}^H\right]\right\|_2 \leq x_{k,n}, \\ y_{k,n}\mathbf{I} - \Theta_k \succeq \mathbf{0}, \\ y_{k,n} \geq 0. \end{cases} \tag{17}$$

Then, Problem $\mathrm{P}_{3-\mathrm{A}}$ is expressed as the following Problem $\mathrm{P}_{3-\mathrm{B}}$ whose constraints are all convex.

$$\begin{aligned} \mathbf{P_{3-B}}: \max_{\left\{\substack{\mathbf{W}_n,\boldsymbol{\Sigma},x_n,y_n,\\ x_{k,n},y_{k,n}}\right\}} &\sum_{n=1}^N R_n\left(\mathbf{W}_n,\boldsymbol{\Sigma}\right) - \lambda P_\mathrm{Total}\left(\mathbf{W}_n,\boldsymbol{\Sigma}\right) \\ \text{s.t. } &(11\mathrm{a}),\ (11\mathrm{b}),\ (16),\ (17), && (18\mathrm{a}) \\ &\mathbf{W}_n \succeq \mathbf{0},\ \boldsymbol{\Sigma} \succeq \mathbf{0},\ \forall n \in \mathcal{N},\ \forall k \in \mathcal{K}. && (18\mathrm{b}) \end{aligned}$$

By defining $R_n\left(\mathbf{W}_n,\boldsymbol{\Sigma}\right) = \omega_n\ \ (n \in \mathcal{N})$, Problem $\mathrm{P}_{3-\mathrm{B}}$ can be further equivalently rewritten as

$$\begin{aligned} \mathbf{P_{3-C}}: \max_{\left\{\substack{\mathbf{W}_n,\boldsymbol{\Sigma},x_n,y_n,\\ x_{k,n},y_{k,n},\omega_n}\right\}} &\sum_{n=1}^N \omega_n - \lambda P_\mathrm{Total}\left(\mathbf{W}_n,\boldsymbol{\Sigma}\right) \\ \text{s.t. } &R_n\left(\mathbf{W}_n,\boldsymbol{\Sigma}\right) \geq \omega_n, && (19\mathrm{a}) \\ &(11\mathrm{a}),\ (11\mathrm{b}),\ (16),\ (17), && (19\mathrm{b}) \\ &\mathbf{W}_n \succeq \mathbf{0},\ \boldsymbol{\Sigma} \succeq \mathbf{0},\ \forall n \in \mathcal{N},\ \forall k \in \mathcal{K}. && (19\mathrm{c}) \end{aligned}$$

It is seen that the main challenge in solving Problem $\mathrm{P}_{3-\mathrm{C}}$ lies in handling (19a) which can be rewritten as

$$\mathbf{h}_n^H\mathbf{W}_n\mathbf{h}_n \geq \left(2^{\omega_n} - 1\right)\left(\sum_{m\neq n}^N \mathbf{h}_n^H\mathbf{W}_m\mathbf{h}_n + \mathbf{h}_n^H\boldsymbol{\Sigma}\mathbf{h}_n + \sigma^2\right).$$

By introducing two more variables, i.e.,

$$\begin{cases} e^{a_n} = \mathbf{h}_n^H\left(\sum_{m\neq n}^n \mathbf{W}_m + \boldsymbol{\Sigma}\right)\mathbf{h}_n, \\ e^{b_n} = 2^{\omega_n} - 1. \end{cases}, \tag{20}$$

and substituting (20) into Problem $\mathrm{P}_{3-\mathrm{C}}$, Problem $\mathrm{P}_{3-\mathrm{C}}$ can be reformulated as the following Problem $\mathrm{P}_{3-\mathrm{D}}$.

$$\begin{aligned} \mathbf{P_{3-D}}: \max_{\left\{\substack{\mathbf{W}_n,\boldsymbol{\Sigma},x_n,y_n,x_{k,n},\\ y_{k,n},a_n,b_n,\omega_n}\right\}} &\sum_{n=1}^N \omega_n - \lambda P_\mathrm{Total}\left(\mathbf{W}_n,\boldsymbol{\Sigma}\right) \\ \text{s.t. } &\mathbf{h}_n^H\mathbf{W}_n\mathbf{h}_n \geq e^{a_n+b_n} + \sigma^2 e^{b_n}, && (21\mathrm{a}) \\ &e^{a_n} \geq \mathbf{h}_n^H\left(\sum_{m\neq n}^n \mathbf{W}_m + \boldsymbol{\Sigma}\right)\mathbf{h}_n, && (21\mathrm{b}) \\ &e^{b_n} \geq 2^{\omega_n} - 1, && (21\mathrm{c}) \\ &(11\mathrm{a}),\ (11\mathrm{b}),\ (16),\ (17), && (21\mathrm{d}) \\ &\mathbf{W}_n \succeq \mathbf{0},\ \boldsymbol{\Sigma} \succeq \mathbf{0},\ \forall n \in \mathcal{N},\ \forall k \in \mathcal{K}. && (21\mathrm{e}) \end{aligned}$$

It can be seen that (21a) is a convex constraint while (21b) and (21c) are not convex. Nevertheless, both the left-hand side parts of (21b) and (21c) are convex functions, i.e., $e^{a_n}$ and $e^{b_n}$. Assuming that $\bar{a}_n$ and $\bar{b}_n$ are the feasible points of Problem $\mathrm{P}_{3-\mathrm{D}}$, the first-order lower bounds of $e^{a_n}$ and $e^{b_n}$ are respectively given by

$$\begin{cases} e^{a_n} \geq e^{\bar{a}_n} + e^{\bar{a}_n}\left(a_n - \bar{a}_n\right), \\ e^{b_n} \geq e^{\bar{b}_n} + e^{\bar{b}_n}\left(b_n - \bar{b}_n\right). \end{cases}$$

Consequently, the restrictive constraints of (21b) and (21c) are respectively given by

$$e^{\bar{a}_n} + e^{\bar{a}_n}\left(a_n - \bar{a}_n\right) \geq \mathbf{h}_n^H\left(\sum_{m\neq n}^n \mathbf{W}_m + \boldsymbol{\Sigma}\right)\mathbf{h}_n \tag{22}$$

and

$$e^{\bar{b}_n} + e^{\bar{b}_n}\left(b_n - \bar{b}_n\right) \geq 2^{\omega_n} - 1. \tag{23}$$

By replacing (21b) and (21c) with (22) and (23), Problem $\mathrm{P}_{3-\mathrm{D}}$ can be approximately formulated as the following Problem $\mathrm{P}_{3-\mathrm{E}}$.

$$\mathbf{P_{3-E}}: \max_{\substack{\{\mathbf{W}_n,\mathbf{\Sigma},x_n,y_n,x_{k,n},\\ y_{k,n},a_n,b_n,\omega_n\}}} \sum\nolimits_{n=1}^{N} \omega_n - \lambda P_{\mathrm{Total}}\left(\mathbf{W}_n,\mathbf{\Sigma}\right)$$
$$\text{s.t. (11a), (11b), (16), (17), (21a), (22), (23),}$$
$$\mathbf{\Sigma} \succeq \mathbf{0},\ \forall n \in \mathcal{N},\ \forall k \in \mathcal{K}.$$

Problem $\mathrm{P}_{3-\mathrm{E}}$ is a convex problem and thus, it can be solved by using standard convex optimization solvers, e.g., SeduMi or CVX [47]. By solving Problem $\mathrm{P}_{3-\mathrm{E}}$, an approximate optimal solution to Problem $\mathrm{P}_{3-\mathrm{D}}$ is obtained at the given $\left\{\bar{a}_n, \bar{b}_n\right\}$. Let $\left\{\mathbf{W}_n^\star, \mathbf{\Sigma}^\star, \omega_n^\star, a_n^\star, b_n^\star\right\}$ be the optimal solution. Since the lower bound in (22) and (23) may not be tight, one have that

$$\begin{aligned}\mathbf{h}_n^H \mathbf{W}_n^\star \mathbf{h}_n &> e^{a_n^\star + b_n^\star} + \sigma^2 e^{b_n^\star} \qquad (25)\\ &> \left(2^{\omega_n^\star} - 1\right)\left(\sum\nolimits_{m\neq n}^{N} \mathbf{h}_n^H \mathbf{W}_m^\star \mathbf{h}_n + \mathbf{h}_n^H \mathbf{\Sigma}^\star \mathbf{h}_n + \sigma^2\right).\end{aligned}$$

That is, the available rate of the $n$-th authorized receiver is strictly larger than $\omega_n$. Therefore, a tighter $\tilde{\omega}_n^\star$ with $\tilde{\omega}_n^\star \geq \omega_n^\star$ for the $n$-th authorized receiver can be obtained by setting

$$\tilde{\omega}_n^\star = \log\left(1 + \frac{\mathbf{h}_k^H \mathbf{W}_n^\star \mathbf{h}_k}{\sum_{m\neq n}^{N} \mathbf{h}_k^H \mathbf{W}_m^\star \mathbf{h}_k + \mathbf{h}_k^H \mathbf{\Sigma}^\star \mathbf{h}_k + \sigma^2}\right).$$

Then, $\left\{\mathbf{W}_n^\star, \mathbf{\Sigma}^\star, \tilde{\omega}_n^\star\right\}$ serves as an approximate solution to Problem $\mathrm{P}_{3-\mathrm{D}}$.

In order to improve the precision of the obtained approximate solution, a SCA-based algorithm is designed as follows. Let $\left\{\mathbf{W}_n^\star(t), \mathbf{\Sigma}^\star(t)\right\}$ be the optimal solution to Problem $\mathrm{P}_{3-\mathrm{E}}$ in the $t$-th iteration. The corresponding $\tilde{\omega}_n^\star(t)$ can be given by

$$\tilde{\omega}_n^\star(t) = \log\left(1 + \frac{\mathbf{h}_n^H \mathbf{W}_n^\star(t)\, \mathbf{h}_n}{\mathbf{h}_n^H \left(\sum_{m\neq n}^{N} \mathbf{W}_m^\star(t) + \mathbf{\Sigma}^\star(t)\right)\mathbf{h}_n + \sigma^2}\right).$$

Then, $\bar{a}_n(t)$ and $\bar{b}_n(t)$ are updated by

$$\begin{cases} \bar{a}_n(t) = \ln\left(\mathbf{h}_n^H \left(\sum_{m\neq n}^{N} \mathbf{W}_m^\star(t) + \mathbf{\Sigma}^\star(t)\right)\mathbf{h}_n\right), \\ \bar{b}_n(t) = \ln\left(2^{\tilde{\omega}_n^\star(t)} - 1\right). \end{cases}$$

By replacing $\bar{a}_n$ and $\bar{b}_n$ in Problem $\mathrm{P}_{3-\mathrm{E}}$ with $\bar{a}_n(t)$ and $\bar{b}_n(t)$, $\left\{\mathbf{W}_n^\star(t+1), \mathbf{\Sigma}^\star(t+1)\right\}$ can be updated by solving the following Problem $\mathrm{P}_{3-\mathrm{F}}$.

$$\mathbf{P_{3-F}}: \max_{\substack{\{\mathbf{W}_n,\mathbf{\Sigma},x_n,y_n,x_{k,n},\\ y_{k,n},a_n,b_n,\omega_n\}}} \sum\nolimits_{n=1}^{N} \omega_n - \lambda P_{\mathrm{Total}}\left(\mathbf{W}_n,\mathbf{\Sigma}\right)$$
$$\text{s.t. } e^{\bar{a}_n(t)} - e^{\bar{a}_n(t)}\left(\bar{a}_n(t) - a_n\right)$$
$$\geq \mathbf{h}_n^H \left(\sum\nolimits_{m\neq n}^{n} \mathbf{W}_m + \mathbf{\Sigma}\right)\mathbf{h}_n \qquad (26a)$$
$$e^{\bar{b}_n(t)} - e^{\bar{b}_n(t)}\left(\bar{b}_n(t) - b_n\right) \geq 2^{\omega_n} - 1 \qquad (26b)$$
$$\text{(11a), (11b), (16), (17), (21a),} \qquad (26c)$$
$$\mathbf{\Sigma} \succeq \mathbf{0},\ \forall n \in \mathcal{N},\ \forall k \in \mathcal{K}. \qquad (26d)$$

In the $(t+1)$-th iteration, $\left\{\mathbf{W}_n^\star(t), \mathbf{\Sigma}^\star(t), \tilde{\omega}_n^\star(t)\right\}$ is a feasible point of Problem $\mathrm{P}_{3-\mathrm{F}}$ and $\tilde{\omega}_n^\star(t+1) \geq \omega_n^\star(t+1)$.

**Algorithm 3** SCA-based algorithm for solving Problem $\mathrm{P}_3$

1: Initialize $\bar{a}_n(0)$ and $\bar{b}_n(0)$,$\forall$n $\in \mathcal{N}$;
2: Set $t = 1$;
3: **repeat**
4: Obtain $\left\{\mathbf{W}_n^\star(t), \mathbf{\Sigma}^\star(t)\right\}$ by solving Problem $\mathrm{P}_{3-\mathrm{F}}$
5: Update $\tilde{\omega}_n^\star(t) = \log\left(1 + \frac{\mathbf{h}_n^H \mathbf{W}_n^\star(t) \mathbf{h}_n}{\mathbf{h}_n^H \left(\sum_{m\neq n}^{N} \mathbf{W}_m^\star(t) + \mathbf{\Sigma}^\star(t)\right)\mathbf{h}_n + \sigma^2}\right)$
6: Update $\bar{a}_n(t) = \ln\left(\mathbf{h}_n^H \left(\sum_{m\neq n}^{N} \mathbf{W}_m^\star(t) + \mathbf{\Sigma}^\star(t)\right)\mathbf{h}_n\right)$ and $\bar{b}_n(t) = \ln\left(2^{\tilde{\omega}_n^\star(t)} - 1\right)$.
7: $t = t + 1$;
8: **until** the stopping criterion is met.
9: Obtain $\mathbf{w}_n^\star$ by rank-one decomposition of $\mathbf{W}_n^\star(t)$ if $\mathrm{Rank}\left(\mathbf{W}_n^\star(t)\right) = 1$; otherwise perform Gaussian randomization [49].
10: Returen $\left\{\mathbf{w}_n^\star, \mathbf{\Sigma}^\star\right\}$.

Thus, we have

$$\begin{aligned}&\sum\nolimits_{n=1}^{N} \tilde{\omega}_n^\star(t+1) - \lambda P_{\mathrm{Total}}\left(\mathbf{W}_n^\star(t+1), \mathbf{\Sigma}^\star(t+1)\right)\\ \geq &\sum\nolimits_{n=1}^{N} \omega_n^\star(t+1) - \lambda P_{\mathrm{Total}}\left(\mathbf{W}_n^\star(t+1), \mathbf{\Sigma}^\star(t+1)\right)\\ \geq &\sum\nolimits_{n=1}^{N} \tilde{\omega}_n^\star(t) - \lambda P_{\mathrm{Total}}\left(\mathbf{W}_n^\star(t), \mathbf{\Sigma}^\star(t)\right),\end{aligned}$$

which means that the optimal result of Problem $\mathrm{P}_{3-\mathrm{F}}$ is increased as the increment of the number of iterations. For clarity, the proposed SCA algorithm is summarized in Algorithm 3.

As the SCA algorithm only guarantees to converge to a stationary point, the approximation accuracy depends on the initial point $\bar{a}_n(0)$ and $\bar{b}_n(0)$. A possible choice is to initialize Algorithm 3 via some heuristic transmission strategies [41]. In this paper, we obtain a feasible solution $\left\{\mathbf{W}_n^\star, \mathbf{\Sigma}^\star\right\}$ by solving Problem $\mathrm{P}_{3-\mathrm{C}}$ with fixed $\{\omega_n\}$, and then, the initial point $\bar{a}_n(0)$ and $\bar{b}_n(0)$ can be obtained by (20).

Combine Algorithm 1, Algorithm 2 and Algorithm 3, the considered Problem $\mathrm{P}_0$ is solved and the optimal GEE can be obtained.

## IV. Discussion of the Effect of AN

It is a fact that the information interception also can be crippled without AN. In this case, the corresponding transmit design can be obtained by solving the non AN-aided design, which is formulated by setting the objective function of Problem $\mathrm{P}_0$ as

$$\max_{\{\mathbf{w}_n,\mathbf{\Lambda}\}} \mathrm{GEE}\left(\mathbf{w}_n\right) = \frac{\sum_{n=1}^{N} \log\left(1 + \frac{\left|\mathbf{h}_n^H \mathbf{w}_n\right|^2}{\sum_{m\neq n}^{N} \left|\mathbf{h}_n^H \mathbf{w}_m\right|^2 + \sigma^2}\right)}{\mu \sum_{n=1}^{N} \left\|\mathbf{w}_n\right\|_2^2 + P_{\mathrm{c}}}$$

and eliminating $\mathbf{\Sigma}$ in (3b)-(3g). Since the non AN-aided design can be considered as a special case of the AN-aided design by setting $\mathbf{\Sigma} = \mathbf{0}$, its corresponding optimization problem can be solved by our proposed solving approach.

To show the effect of AN, in this following proposition, we prove that the GEE can be improved by employing AN.

**Proposition 1.** *The maximum GEE obtained by the AN-aided design shall not be less than that obtained by the non AN-aided design under the same condition.*

*Proof:* It is seen that the optimal solution to the non AN-aided design is a feasible solution to the AN-aided design with $\mathbf{\Sigma} = \mathbf{0}$. So, the optimal result, i.e., maximum GEE, of the AN-aided design shall be larger than or equal to that of non AN-aided design, which means the GEE obtained by the AN-aided design shall not be less than that obtained by the non AN-aided design. ■

The maximum GEE obtained by the AN-aided design is equal to that obtained by the non AN-aided design only when the optimal $\mathbf{\Sigma}$ of the AN-aided design equal to $\mathbf{0}$. In our considered system, AN not only cripples the information interception but also plays a role as energy carrier, which could hardly reduce to $\mathbf{0}$. Thus, in most cases, the GEE obtained by the AN-aided design is larger than that obtained by the non AN-aided design. This result is consistent with the analysis in [23].

## V. Numerical Results

This section provides some simulation results to discuss the system GEE performance behaviors. For comparison, the sum-rate maximization design, the power minimization design, the GEE maximization design under sum-rate constraint, the non-robust design, the non AN-aided design and traditional linear EH model based design are also simulated. In order to show the efficiency of our proposed solving approach, the convergency is also discussed via simulations.

The simulated scenario is shown in Figure 1. The authorized receivers and the idle receivers are positioned at a distance of $10\mathrm{m}$ and $5\mathrm{m}$ from the transmitter, respectively. For the transmitter, the number of the transmit antenna $N_{\mathrm{T}}$ is set as 3. The power amplifier efficiency factor $\mu$ and the circuit power consumption $P_{\mathrm{c}}$ are set as 5 and $0.1\mathrm{W}$, respectively. The total available power $P_{\mathrm{Max}}$ is set as 2W. The numbers of authorized receivers $N$ and idle receivers $K$ are all set as 2. The noise power spectral density is $-162\mathrm{dBm/Hz}$ and the bandwidth $B$ is 10MHz. The channel model adopted in our simulation is given by (i.e., [50])

$$\mathbf{h}_n = \mathrm{PL}\left(d_n\right) \cdot \psi_n \cdot \varphi \cdot \hat{\mathbf{h}}_n \text{ and } \mathbf{g}_k = \mathrm{PL}\left(d_k\right) \cdot \psi_k \cdot \varphi \cdot \hat{\mathbf{g}}_k$$

where $\mathrm{PL}\left(d\right) = 10^{-(128.1+37.6\log_{10}(d))/20}$, $d_n$ and $d_k$ denote the distance between the transmitter and the $n$-th authorized receiver and the $k$-th unauthorized receiver, respectively. $\psi_n$ and $\psi_k$ represent their shadow fading, which follows the log-normal distribution with zero mean and standard deviation 8. $\varphi$ denotes the transmit-receive antenna gain which is set to $15\mathrm{dBi}$, and $\hat{\mathbf{h}}_n$ and $\hat{\mathbf{g}}_k$ are the small scale fading which follows complex Gaussian random variable with zero mean and unit variance. The minimum required rate of each authorized receiver is set as 1bits/Hz, i.e., $R_n^{(\mathrm{D})} = R^{(\mathrm{D})} = 1\mathrm{bits/Hz}$ $\forall n \in \mathcal{N}$. The EH power requirement at each idle receiver is set as $20\mathrm{mW}$, i.e., $\theta_k = 20\mathrm{mW}$ $\forall k \in \mathcal{K}$. The secure SINR threshold $\Gamma_{\mathrm{E}}$ is set as $0\mathrm{dB}$. For the SUM, the CSI errors are assumed to be spatial i.i.d. and have standard circularly symmetric complex Gaussian distribution $\mathbf{C}_k = \mathbf{C}_k = \nu^2\mathbf{I}_{N_{\mathrm{T}}}$, and $\nu^2 = 0.002$. The maximum outage probability for EH and the maximum tolerable probability for information leakage for each idle receiver are set the same, i.e., $p_k^{(\mathrm{EH})} = p_{k,n}^{(\mathrm{ID})} = 0.01$. For the PS EH receiver architecture, we set $L = 4$. For the non-linear EH model, we set $M_{kl}$ as $24\mathrm{mW}$ which corresponds to the maximum harvested power at each authorized receiver. Besides, we adopt $\upsilon_{kl}$ = 150 and $\varphi_{kl}$ = 0.024. All parameters described above in the simulations will not change as unless otherwise specified.

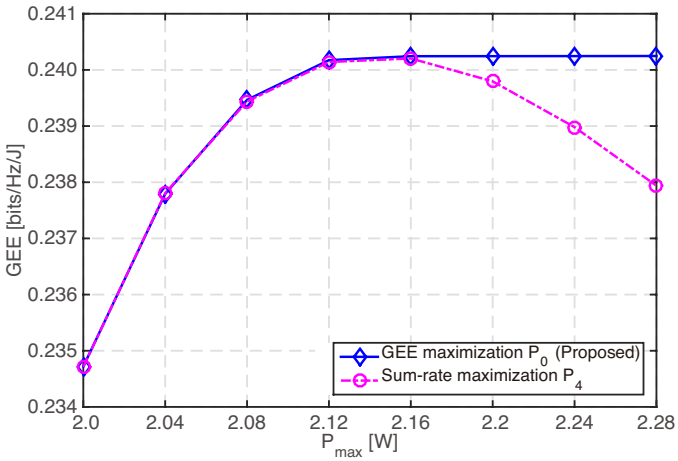


Fig. 5. GEE Maximization versus $P_{\mathrm{Max}}$.

### A. GEE Maximization versus $P_{\mathrm{Max}}$

In this subsection, we show the the GEE maximization versus $P_{\mathrm{Max}}$. For comparison, sum-rate maximization system design is also studied, which is formulated as following Problem $\mathrm{P}_4$.

$$\mathbf{P_4}: \max_{\{\mathbf{w}_n, \mathbf{\Sigma}, \mathbf{\Lambda}\}} \sum\nolimits_{n=1}^{N} R_n\left(\mathbf{w}_n, \mathbf{\Sigma}\right) \tag{27a}$$

$$\text{s.t. } (3\mathrm{c}),\ (3\mathrm{d}),\ (3\mathrm{e}),\ (3\mathrm{f}),\ (3\mathrm{g}). \tag{27b}$$

It can be seen that Problem $\mathrm{P}_4$ has a very similar form to Problem $\mathrm{P}_3$, so it can be efficiently solved by our proposed Algorithm 3. The simulation results are presented in Figure 5. It is observed that the GEE obtained by the sum-rate maximization design first increases and then decreases with the increment of $P_{\mathrm{Max}}$ while the GEE of the proposed GEE maximization design does not decrease, because wireless communication is bandwidth and power limited. When it works in the power-limited region, the obtained profit in terms of information rate by consuming the power decreases. Therefore, for the GEE maximization design, there exists a $P_{\mathrm{Max}}$ threshold, when $P_{\mathrm{Max}}$ is larger than the threshold, the total required power of the GEE maximization design keeps unchanged, while for the sum-rate maximization design, as all available power, i.e., $P_{\mathrm{Max}}$, is consumed, it degrades the GEE when $P_{\mathrm{Max}}$ is larger than the threshold. Moreover, it is noticed that when $P_{\mathrm{Max}}$ is less the threshold, the GEE maximization design and the sum-rate maximization design achieve the similar system GEE. The reason is that, when

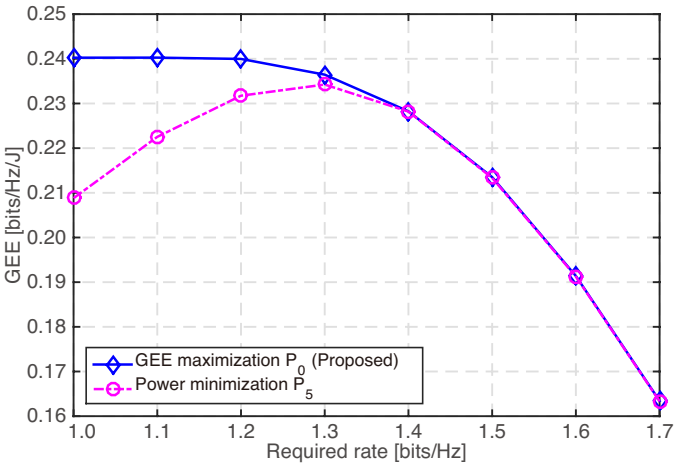


Fig. 6. GEE maximization versus $R^{(\mathrm{D})}$.

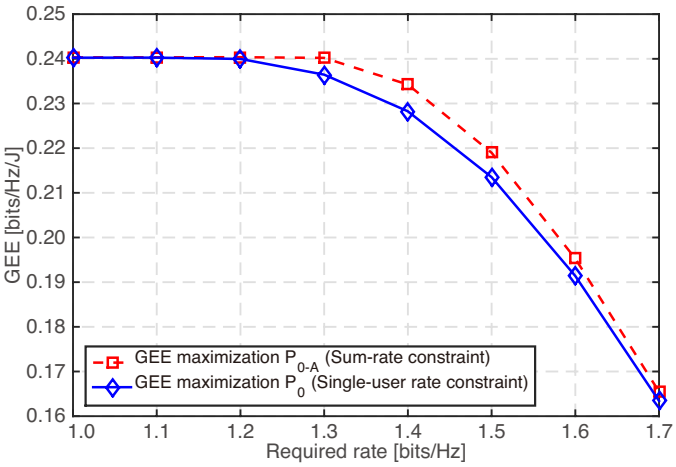


Fig. 7. GEE under single-user rate constraint versus that under sum-rate constraint.

$P_{\mathrm{Max}}$ is smaller than the threshold, all available power is used in both designs. In this case, although sum-rate maximization aims to maximize the system rate, its power is fully utilized, so it also achieves the optimal GEE.

### B. GEE Maximization versus $R^{(\mathrm{D})}$

In this subsection, we show the GEE maximization versus $R^{(\mathrm{D})}$. For comparison, power minimization system design is also studied, which is formulated as following Problem $\mathrm{P}_5$.

$$\mathbf{P_5}: \min_{\{\mathbf{w}_n,\mathbf{\Sigma},\mathbf{\Lambda}\}} P_{\mathrm{Total}}\left(\mathbf{w}_n,\mathbf{\Sigma}\right) \tag{28a}$$

$$\text{s.t. } (3\mathrm{b}),\ (3\mathrm{d}),\ (3\mathrm{e}),\ (3\mathrm{f}),\ (3\mathrm{g}). \tag{28b}$$

Problem $\mathrm{P}_5$ can be solved based on SDR and Bernstein-type inequality, and the detailed process of solution method can be found in Appendix A. The simulation results are plotted in Figure 6. It is observed that the GEE obtained by the power minimization design first increases and then decreases with increment of $R^{(\mathrm{D})}$ while the GEE of the proposed GEE maximization design first keeps unchanged and then decreased. The reason is that in the power minimization design, the total required power is minimized to satisfy the minimal rate constraints while in the GEE maximization design, the total required power is minimized and the sum rates are maximized at the same time. That is, the minimal rate constraints may be tight in power minimization design while they may not be tight in the GEE maximization design, which means that higher sum rates are achieved by the GEE maximization design. Moreover, it is noticed that when $R^{(\mathrm{D})}$ is relatively large, the GEE maximization design and the power minimization design achieve the similar system GEE. The reason might be that in this case, the minimal total required power by both designs may be similar, and at the same time, the guaranteed minimal rate, i.e, $R^{(\mathrm{D})}$, of the power minimization design is also similar to the maximal rate achieved by the GEE maximization design for each authorized receiver.

### C. GEE under Single-User Rate Constraint versus that under Sum-Rate Constraint

Problem $\mathrm{P}_0$ is actually with the single-user rate constraint, i.e., (3b). For better understanding of the system performance, we also considered and simulated the GEE maximization design under another type of QoS constraints, i.e., the sum-rate constraint, which means that the sum rates of all authorized receivers are larger than a pre-defined threshold. For fair comparison with single-user rate constraint, the threshold is set as $\sum_{n=1}^{N} R_n^{(\mathrm{D})}$ and the corresponding problem is formulated as following Problem $\mathrm{P}_{0-\mathrm{A}}$.

$$\mathbf{P_{0-A}}: \max_{\{\mathbf{w}_n,\mathbf{\Sigma},\mathbf{\Lambda}\}} \mathrm{GEE}\left(\mathbf{w}_n,\mathbf{\Sigma}\right) \tag{29a}$$

$$\text{s.t. } \sum\nolimits_{n=1}^{N} R_n\left(\mathbf{w}_n,\mathbf{\Sigma}\right) \geq \sum\nolimits_{n=1}^{N} R_n^{(\mathrm{D})}, \tag{29b}$$

$$(3\mathrm{c}),\ (3\mathrm{d}),\ (3\mathrm{e}),\ (3\mathrm{f}),\ (3\mathrm{g}). \tag{29c}$$

Problem $\mathrm{P}_{0-\mathrm{A}}$ can be solved by the proposed solving approach. The simulation results are presented in Figure 7. One can observe that the GEE maximization design with sum-rate constraint, i.e., (29b), achieves larger GEE than the GEE maximization design with single-rate constraint, i.e., (3b). The reason is that when the sum-rate constraint is considered, the resource will be allocated to the receivers with relatively good channel condition preferentially. In this case, the single-rate constraint may not hold for receivers with poor channel condition and thus, the fairness among users may not be guaranteed. From the mathematical perspective, (29b) holds if (3b) is satisfied but the converse is not necessarily true. That is, (3b) is a sufficient but not necessary for (29b).

### D. The Effect of AN on System GEE

Figure 8 compares the proposed AN-aided robust design with the non AN-aided robust design. Besides, the result of the AN-aided non-robust design is also given as a benchmark where the CSI of the idle receivers is regard to be perfectly known at the transmitter. It is observed that with the increment of number of antennas, the GEE of all three designs increases

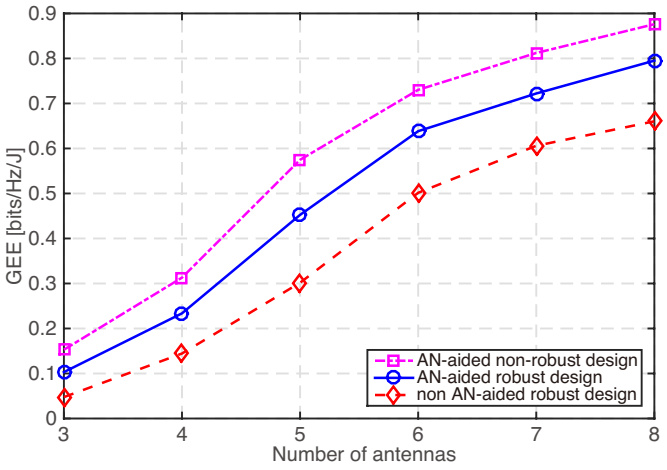


Fig. 8. Comparison of proposed AN-aided design and non AN-aided design.

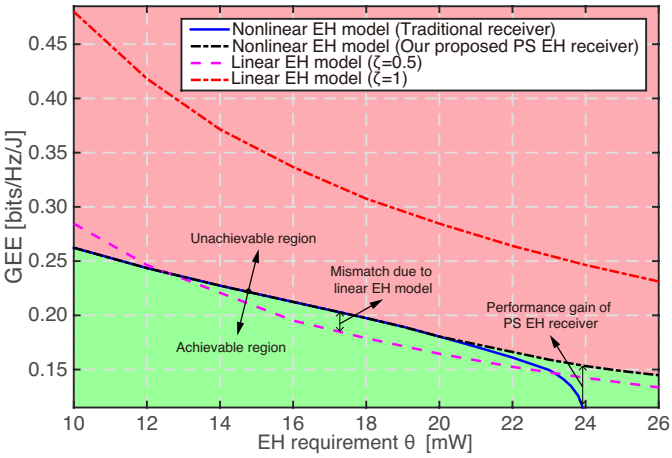


Fig. 9. Comparison of non-linear EH model and linear EH model in terms of GEE.

because more antennas yield larger spatial DoF to transmit information and energy. Compared with the non AN-aided robust design, the proposed AN-aided robust design is able to achieve larger GEE, which is consistent with Proposition 1. One can also see that the AN-aided non-robust design achieve higher GEE than the proposed AN-aided robust design. The reason is that for the robust design, due to the CSI errors, the transmitter need to generate "wider" beams to satisfy the system requirements which required more power. Nevertheless, it is by no means that the non-robust design is superior to the robust design. Although higher GEE is achieved by the non-robust design, it cannot always satisfy the system requirements when CSI involves errors. Moreover, the non-robust design can be regarded as a special case of the robust design where the CSI errors are set as $\mathbf{0}$.

### *E. Performance Behavior of Our Proposed PS EH Receiver Architecture*

An example to show performance behavior of the proposed PS EH receiver architecture is given by Table I where the input RF power is 50mW. It is seen that by the proposed PS EH receiver architecture and PS ratio assignment, the output DC power increases from 19.9mW to 33.0mW which means that the RF-DC conversion efficiency increases from $38.8\%$ to $66.0\%$. The reason is that in the relatively high input RF power level, the reverse breakdown voltage of the diode decreases the RF-DC conversion efficiency as shown in Figure 2(b). By the proposed PS EH receiver architecture, the input RF power is spitted into $L$ streams and each stream is input into one EH circuit. As the power of each stream is smaller than the total one, with the proposed PS ratio assignment, each EH circuit can be guaranteed working in the non-saturation region. Another example with input RF power being 30mW is given by Table II. It is observed that the optimal output DC power can be achieved at last $L = 2$ and the optimal output DC power keep unchanged as $L$ increasing. The reason is that in this case, the PS ratios optimized by Algorithm 1 do not change when $L \geq 0$.

TABLE I
PERFORMANCE BEHAVIOR OF OUR PROPOSED PS EH RECEIVER ARCHITECTURE WHEN INPUT RF POWER IS 50MW

| Number of EH circuits $L$ | 1 | 2 | 3 | 4 |
|---|---|---|---|---|
| Output DC power (mW) | 19.9 | 32.8 | **33.0** | **33.0** |

TABLE II
PERFORMANCE BEHAVIOR OF OUR PROPOSED PS EH RECEIVER ARCHITECTURE WHEN INPUT RF POWER IS 30MW

| Number of EH circuits $L$ | 1 | 2 | 3 | 4 |
|---|---|---|---|---|
| Output DC power (mW) | 18.1 | **19.2** | **19.2** | **19.2** |

Figure 9 compares the non-linear EH model with traditional linear EH model w.r.t. GEE, where for the linear EH model, the RF-DC conversion efficiency $\zeta$ is set as $0.5$ and $1$, respectively. It is observed that the GEE of both non-linear and linear EH models decreases with the increment of EH requirement. The reason is that the increment of EH requirement only increases the total required power but not increases the sum rate of the authorized receivers which degrades the GEE. Different from traditional linear EH model, when the EH requirement approach the maximum output DC power (e.g., $M = 24$mW in this example), the GEE of the non-linear EH model with traditional EH receiver architecture decreases sharply. However, with the proposed PS EH receiver architecture, the maximum limitation on the output DC power of EH circuits is broke and therefore, the GEE is improved.

Figure 10 compares the non-linear EH model with traditional linear EH model w.r.t. the total required power at the transmitter. It is observed that for the linear EH model, the total required power increases as the EH power requirement increases. While for the non-linear EH model, the total required power also increases as the EH power requirement increases, but there exists a saturation point on the EH power requirement (e.g., $M = 24$mW in this example) when the traditional receiver architecture is adopted because of the non-linear EH circuit feature. With the proposed PS EH receiver architecture, the EH power requirement can surpass the saturation point.

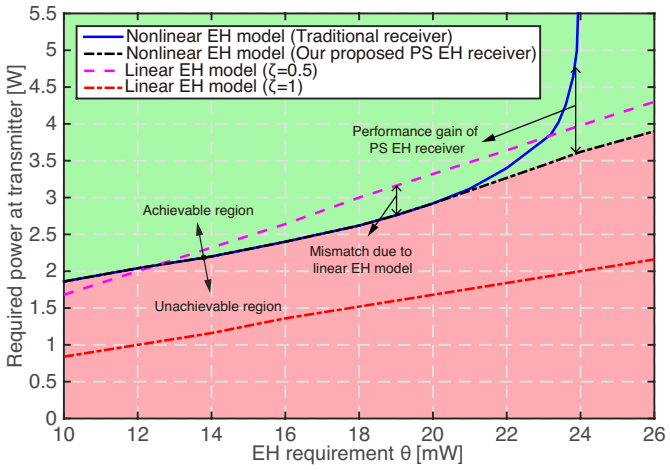


Fig. 10. Comparison of non-linear EH model and linear EH model in terms of $P_{\text{Total}}$.

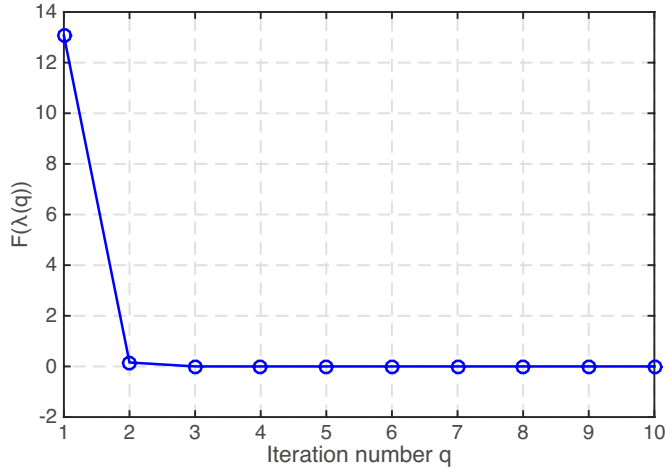


Fig. 11. Convergence behavior of Algorithm 2.

Moreover, if the linear EH model with $\zeta = 1$ is adopted, it may result in false and deceptive output DC power. That is, although less power is consumed by the linear EH model, the output DC power cannot meet the practical requirement (i.e., (3d) cannot be satisfied). Thus, the false output DC power is avoided by employing the non-linear EH model.

### *F. Convergence Performance of the Proposed Solving Approach*

For the proposed solving approach, the computational complexity is mainly due to Algorithm 2. Figure 11 gives the convergence behavior of Algorithm 2. It is seen that as the iteration number $q$ increasing, $F(\lambda(q))$ converges to be 0. In Algorithm 2, $F(\lambda(q)) = 0$ indicates $\sum_{n=1}^{N} R_n(\mathbf{w}_n^\star(q), \mathbf{\Sigma}^\star(q)) = \lambda(q) P_{\text{Total}}(\mathbf{w}_n^\star(q), \mathbf{\Sigma}^\star(q))$ and thus, the optimal GEE, i.e., $\lambda(q)$, is numerically obtained. One can also observe that the converge speed is fast in this example where only 4 steps is required.

In Algorithm 2, each iteration includes a subproblem which is solved by Algorithm 3. Figure 12 shows convergence of

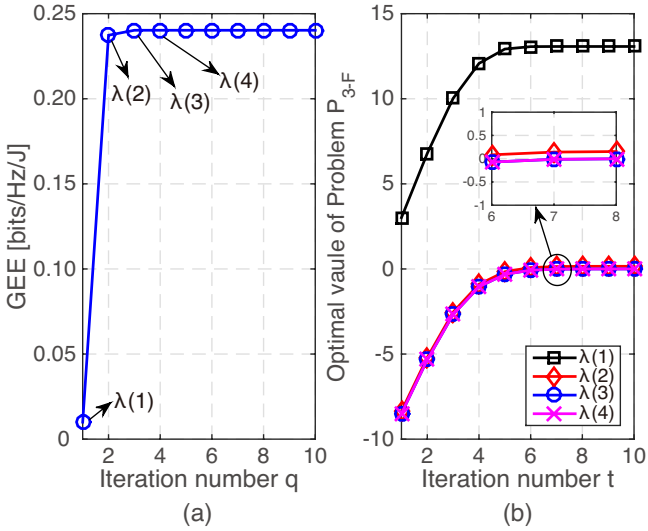


Fig. 12. (a) Convergence of GEE, i.e., $\lambda$. (b) Convergence behavior of Algorithm 3.

GEE obtained by Algorithm 2 and the convergence behavior of Algorithm 3. It is seen that Algorithm 3 converges for a given $\lambda$, and as $\lambda$ increasing, the optimal result of Algorithm 3 decreases. Combine with Figure 11 and Figure 12, one can see the relationship between Algorithm 2 and Algorithm 3 is that in each iteration of Algorithm 3, the objective function of Problem $\mathrm{P}_{3-\mathrm{F}}$ is actually $F(\lambda(q))$. Thus, when Algorithm 3 converges to 0, $F(\lambda(q)) = 0$ is obtained and the stopping criterion of Algorithm 2 is met.

## VI. Conclusion

This paper investigated system GEE for secure MISO SWIPT systems. The non-linear EH model was employed and a novel PS EH receiver architecture was proposed. A GEE maximization problem was formulated to satisfy the minimal rate requirement and the secure transmission constraints of authorized receivers, the EH requirements of idle receivers and the total available power constraint at the transmitter. An efficient solving approach was designed to solve the problem. Firstly, the PS ratios were optimized by using bisection method and SCA. Then, an iterative solution framework based on Dinkelbach's algorithm was presented to jointly optimize the transmit beamforming vectors and the AN covariance matrix, where a SCA-based algorithm was designed to solve its non-convex subproblem. Numerous simulation results showed that compared with the sum-rate maximization design and power minimization design, the proposed GEE maximization design is able to achieve better system performance. Compared with traditional EH receiver architecture and linear EH model, the proposed PS EH receiver architecture is able to achieve higher system GEE and avoid false output power at idle receivers.

## Appendix A
## Solution Method for Problem $\mathrm{P}_5$

Similar to the proposed solving approach in Section III, we first optimize $\mathbf{\Lambda}$ by Algorithm 1. Then, with $\mathbf{\Lambda}^\star$ and $\mathcal{E}_k^\star$, we

optimize $\{\mathbf{w}_n, \mathbf{\Sigma}\}$ by solving the following Problem $\mathrm{P}_{5-\mathrm{A}}$ instead of Problem $\mathrm{P}_5$.

$$\mathbf{P_{5-A}}: \min_{\{\mathbf{w}_n, \mathbf{\Sigma},\}} P_{\mathrm{Total}}\left(\mathbf{w}_n, \mathbf{\Sigma}\right) \tag{30a}$$

$$\text{s.t. } (3\mathrm{b}),\ (10\mathrm{b}),\ (3\mathrm{e}),\ (3\mathrm{g}). \tag{30b}$$

By SDR and Bernstein-type inequality, Problem $\mathrm{P}_{5-\mathrm{A}}$ can be transferred into the following Problem $\mathrm{P}_{5-\mathrm{B}}$.

$$\mathbf{P_{5-B}}: \min_{\{\mathbf{W}_n, \mathbf{\Sigma},\}} P_{\mathrm{Total}}\left(\mathbf{W}_n, \mathbf{\Sigma}\right) \tag{31a}$$

$$\text{s.t. } (11\mathrm{a}),\ (16),\ (17),\ (11\mathrm{e}). \tag{31b}$$

Problem $\mathrm{P}_{5-\mathrm{B}}$ is a convex problem and thus, it can be solved by using standard convex optimization solvers and $\{\mathbf{W}_n^\star, \mathbf{\Sigma}^\star\}$ is derived. As the goal of Problem $\mathrm{P}_5$ is to find $\{\mathbf{w}_n^\star\}$ rather than $\{\mathbf{W}_n^\star\}$. Thus, once we get $\{\mathbf{W}_n^\star\}$, we have to recover the corresponding $\{\mathbf{w}_n^\star\}$. If $\mathrm{Rank}\left(\mathbf{W}_n^\star\right) = 1$, $\mathbf{w}_n^\star$ can be derived by rank-one decomposition of $\mathbf{W}_n^\star$. Otherwise, $\mathbf{w}_n^\star$ can be approximately derived by Gaussian randomization procedure.

## REFERENCES


[1] R. Zhang and C. Ho, "MIMO broadcasting for simultaneous wireless information and power transfer," *IEEE Trans. Wirel. Commun.*, vol. 12, no. 5, pp. 1989-2001, May 2013.

[2] X. Lu, P. Wang, D. Niyato, D. I. Kim, and Z. Han, "Wireless network with RF energy harvesting: A contemporary survey," *IEEE Commun. Surveys Tuts.*, vol. 17, no. 2, pp. 757-789, Nov. 2015.

[3] I. Krikidis, S. Timotheou, S. Nikolaou, G. Zheng, D. W. K. Ng, and R. Schober, "Simultaneous wireless information and power transfer in modern communication systems," *IEEE Commun. Mag.*, vol. 52, no. 11, pp.104-110, Nov. 2014.

[4] B. Clerckx, "Wireless information and power transfer: Nonlinearity, waveform design and rate-energy tradeoff," *IEEE Trans. Signal Process.*, vol 66, no 4, pp. 847-862, Feb 2018.

[5] M.-L. Ku, W. Li, Y. Chen, and K. J. R. Liu, "Advances in energy harvesting communications: past, present, and future challenges," *IEEE Commun. Surveys Tuts.*, vol. 18, no. 2, pp. 1384-1412, 2015.

[6] F. Benkhelifa, A. Sultan Salem, and M.-S. Alouini, "Sum-rate enhancement in multiuser MIMO decode-and-forward relay broadcasting channel with energy harvesting relays," *IEEE J. Sel. Areas Commun.*, vol. 34, no. 12, pp. 3675-3684, Sept. 2016.

[7] Y. Liu, Z. Ding, M. Elkashlan, and H. V. Poor, "Cooperative non-orthogonal multiple access with simultaneous wireless information and power transfer," *IEEE J. Sel. Areas Commun.*, vol. 34, no. 4, pp. 938-953, Mar. 2016.

[8] J. Huang, C.-C. Xing, and C. Wang, "Simultaneous wireless information and power transfer: Technologies, applications, and research challenges," *IEEE Commun. Mag.*, vol. 55, no. 11, pp. 26-32, Nov. 2017.

[9] F. Akhtar and M. H. Rehmani, "Energy harvesting for self-sustainable wireless body area networks," *IT Prof.*, vol. 19, no. 2, pp. 32-40, Apr. 2017.

[10] Q. Li and W.-K. Ma, "Spatially selective artificial-noise aided transmit optimization for MISO multi-Eves secrecy rate maximization," *IEEE Trans. Signal Process.*, vol. 61, no. 10, pp. 2704-2717, May 2013.

[11] D. W. K. Ng, E. S. Lo and R. Schober, "Robust beamforming for secure communication in systems with wireless information and power transfer," *IEEE Trans. Wirel. Commun.*, vol. 13, no. 8, pp. 4599-4615, Aug. 2014.

[12] C. Han etc., "Green radio: radio techniques to enable energy-efficient wireless networks," *IEEE Commun. Mag.*, vol. 49, no. 6, pp.104-110, June 2011.

[13] S. Buzzi, C.-L. I, T. E. Klein, H. V. Poor, C. Yang, and A. Zappone, "A survey of energy-efficient techniques for 5G networks and challenges ahead," *IEEE J. Sel. Areas Commun.*, vol. 34, no. 4, pp. 697-709, Apr. 2016.

[14] S. D. Muruganathan, D. C. F. Ma, R. I. Bhasin, and A. O. Fapojuwo, "A centralized energy-efficient routing protocol for wireless sensor network," *IEEE Commun. Mag.*, vol. 52, no. 11, pp.104-110, Nov. 2014.

[15] M. Sheng, Y. Li, X. Wang, J. Li, and Yan Shi, "Energy efficiency and delay tradeoff in device-to-device communications underlaying cellular networks," *IEEE J. Sel. Areas Commun.*, vol. 34, no. 1, pp. 92-106, Jan. 2016.

[16] D. W. K. Ng, E. S. Lo, and R. Schober, "Energy-efficient resource allocation in multi-cell OFDMA systems with limited backhaul capacity," *IEEE Trans. Wireless Commun.*, vol. 11, no. 10, pp. 3618-3631, Sept. 2012.

[17] D. W. K. Ng, E. S. Lo, and R. Schober, "Wireless information and power transfer: energy efficiency optimization in OFDMA systems," *IEEE Trans. Wireless Commun.*, vol. 12, no. 12, pp. 6352-6370, Nov. 2013.

[18] Q. Shi, M. Razaviyayn, Z. Q. Luo, and C. He, "An iteratively weighted MMSE approach to distributed sum-utility maximization for a MIMO interfering broadcast channel," *IEEE Trans. Signal Process.*, vol. 59, no. 9, pp. 4331-4340, Sept. 2011.

[19] Y. Lu, K. Xiong, P. Y. Fan, and Z. D. Zhong, "Optimal multicell coordinated beamforming for downlink high-speed railway communications," *IEEE Trans. Veh. Technol.*, vol. 66, no. 10, pp. 9603-9608, Jun. 2017.

[20] L. Liu, R. Zhang, and K.-C. Chua, "Secrecy wireless information and power transfer with MISO beamforming," *IEEE Trans. Signal Process.*, vol. 62, no. 7, pp. 1850-1863, Jan. 2014.

[21] Q. Li, Q. Zhang, and J. Qin, "Secure relay beamforming for simultaneous wireless information and power transfer in nonregenerative relay networks," *IEEE Trans. Veh. Technol.*, vol. 63, no. 5, pp. 2462-2467, Jan. 2014.

[22] F. H. Zhou, Z. Li, J. L. Cheng, Q. W. Li, and J. B. Si, "Robust AN-aided beamforming and power splitting design for secure MISO cognitive radio with SWIPT," *IEEE Trans. Wirel. Commun.*, vol. 16, no. 4, pp. 2450-2464, Mar. 2017.

[23] Y. Lu, K. Xiong, P. Y. Fan, Z. D. Zhong, and K. B. Letaief, "Robust transmit beamforming with artificial redundant signals for secure SWIPT systems under non-linear EH model," *IEEE Trans. Wireless Commun.*, vol. PP, no. 99, pp. 1-1, Jan. 2018.

[24] S. Guo, F. Wang, Y. Yang, and B. Xiao, "Energy-efficient cooperative transmission for simultaneous wireless information and power transfer in clustered wireless sensor networks," *IEEE Trans. Commun.*, vol. 63, no. 11, pp. 4405-4417, Sept. 2015.

[25] Y. Zhao, V. C. M. Leung, C. Zhu, H. Gao, Z. Chen, and H. Ji, "Energy-efficient sub-carrier and power allocation in cloud-based cellular network with ambient RF energy harvesting," *IEEE Access*, vol. 5, pp. 1340-1352, Feb. 2017.

[26] C. You, K. Huang, and H. Chae, "Energy efficient mobile cloud computing powered by wireless energy transfer," *IEEE J. Sel. Areas Commun.*, vol. 34, no. 5, pp. 1757-1771, Mar. 2016.

[27] M. Sheng, L. Wang, X. Wang, Y. Zhang, C. Xu, and J. Li, "Energy efficient beamforming in MISO heterogeneous cellular networks with wireless information and power transfer," *IEEE J. Sel. Areas Commun.*, vol. 34, no. 4, pp. 954-968, Apr. 2016.

[28] J. Rostampoor, S. M. Razavizadeh, and I. Lee, "Energy efficient precoding design for SWIPT in MIMO two-way relay networks," *IEEE Trans. Veh. Technol.*, Vol. 66, no. 9, pp. 7888-7896, Sept. 2017.

[29] W. Mei, Z. Chen, and J. Fang, "Artificial noise aided energy efficiency optimization in MIMOME system with SWIPT," *IEEE Commun. Lett.*, vol. 21, no. 8, pp. 1795-1798, Apr. 2017.

[30] A. A. Nasir, H. D. Tuan, T. Q. Duong, and H. V. Poor, "Secure and energy-efficient beamforming for simultaneous information and energy transfer," *IEEE Trans. Wireless Commun.*, vol. PP, no. 99, pp. 7523-7537, Nov. 2017.

[31] J. Zhang and G. Pan,"Outage analysis of wireless-powered relaying MIMO systems with non-linear energy harvesters and imperfect CSI," *IEEE Access*, vol. 4, pp. 7046-7053, Oct. 2016.

[32] E. Boshkovska, D. W. K. Ng, N. Zlatanov, A. Koelpin, and R. Schober, "Robust resource allocation for MIMO wireless powered communication networks based on a non-linear EH model," *IEEE Trans. Wirel. Commun.*, vol. 65, no. 5, pp. 1984-1999, May 2017.

[33] B. Clerckx and E. Bayguzina, "Waveform design for wireless power transfer," *IEEE Trans. Signal Process.*, Vol. 64, No. 23, pp. 6313-6328, Dec. 2016.

[34] Y. Huang and B. Clerckx, "Waveform design for wireless power transfer with limited feedback," *IEEE Trans. Wirel. Commun.*, vol 17, no 1, pp. 415-429, Jan. 2018.

[35] B. Clerckx, E. Bayguzina, D. Yates, and P. D. Mitcheson, "Waveform optimization for wireless power transfer with nonlinear energy harvester modeling, *IEEE ISWCS*, pp. 276-280, 2015.

[36] C. R. Valenta and G. D. Durgin, "Harvesting wireless power: Survey of energy-harvester conversion efficiency in far-field, wireless power transfer systems," *IEEE Microw. Mag.*, vol. 15, no. 4, pp. 108-120, May 2014.

[37] K. G. Nguyen, Q. D. Vu, M. Juntti, and L. N. Tran, "Distributed solutions for energy efficiency fairness in multicell MISO downlink," *IEEE Trans. Wireless Commun.*, vol. 16, no. 9, pp. 6232-6247, Oct. 2017.

[38] O. Tervo, L.-M. Tran, and M. Juntti, "Optimal energy-efficient transmit beamforming for multi-user MISO downlink," *IEEE Trans. Signal Process.*, vol. 63, no. 20, pp. 5574-5588, Oct. 2015.

[39] Y. Huang, S. He, S. Jin, and W. Chen, "Decentralized energy-efficient coordinated beamforming for multicell systems," *IEEE Trans. Veh. Technol.*, vol. 63, no. 9, pp. 4302-4314, Mar. 2014.

[40] A. Zappone, P. Cao, and E. A. Jorswieck, "Energy efficiency optimization in relay-assisted MIMO systems with perfect and statistical CSI," *IEEE Trans. Signal Process.*, vol. 62, no. 2, pp. 443-457, Jan. 2014.

[41] W.-C. Li, T.-H. Chang, C. Lin, and C.-Y. Chi, "Coordinated beamforming for multiuser MISO interference channel under rate outage constraints," *IEEE Trans. Signal Process.*, vol. 61, no. 5, pp. 1087-1103, Nov. 2012.

[42] W. Dinkelbach, "On nonlinear fractional programming," *Manage. Sci.*, vol. 13, no. 7, pp. 492-498, Mar. 1967.

[43] A. Zappone and E. Jorswieck, "Energy efficiency in wireless networks via fractional programming theory," *Found. Trends Commun. Inf. Theory*, vol. 11, no. 3-4, pp. 185-396, 2015.

[44] C. Isheden, Z. Chong, E. Jorswieck, and G. Fettweis, "Framework for link-level energy efficiency optimization with informed transmitter," *IEEE Trans. Wireless Commun.*,vol. 11, no. 8, pp. 2946-2957, Aug. 2012.

[45] A. Zappone, E. Bjrnson, L. Sanguinetti, and E. Jorswieck, "Globally optimal energy-efficient power control and receiver design in wireless networks," *IEEE Trans. Signal Process.*, vol. 65, no. 11, pp. 2844-2859, June 2017.

[46] A. Pascual-Iserte, D. P. Palomar, A. I. Perez-Neira, and M. A. Lagunas, "A robust maximin approach for MIMO communications with imperfect channel state information based on convex optimization," *IEEE Trans. Signal Process.*, vol. 54, no. 1, pp. 346-360, Jan. 2006.

[47] S. Boyd and L. Vandenberghe, Convex Optimization. Cambridge, U.K.: Cambridge Univ. Press, 2004.

[48] K.-Y. Wang, A. M.-C. So, T.-H. Chang, W.-K. Ma, and C.-Y. Chi, "Outage constrained robust transmit optimization for multiuser MISO downlinks: Tractable approximations by conic optimization," *IEEE Trans. Signal Process.*, vol. 62, no. 21, pp. 5690-5705, Sep. 2014.

[49] Z.-Q. Luo, W.-K. Ma, A. M.-C. So, Y. Ye, and S. Zhang, "Semidefinite relaxation of quadratic optimization problems," *IEEE Signal Process. Mag.*, vol. 27, no. 3, pp. 20-34, May 2010.

[50] H. Dahrouj and W. Yu, "Coordinated beamforming for the multicell multi-antenna wireless system," *IEEE Trans. Wirel. Commun.*, vol. 9, no. 5, pp. 1748-1759, May 2010.